PRECISION LASER SPECTROSCOPY USING ACOUSTO-OPTIC MODULATORS

W. A. VAN WIJNGAARDEN
Physics Department, York University
Toronto, Ontario, Canada

I. Introduction

Precision optical spectroscopy is an invaluable tool to study atomic structure. Absolute measurements of optical transition frequencies can be readily made with an accuracy of parts in 10^9 (Riis *et al.*, 1994). However, in many experiments one is primarily interested in determining the energy interval separating two nearby states. Examples include fine and hyperfine structure splittings, isotope shifts, and the Lamb shift. Additional frequency shifts arise when electric and magnetic fields are applied to the atom. These energy splittings can be found by subtracting precisely determined frequencies of transitions occurring to the states in question. For

ISBN 0-12-003836-6

example, consider an atom that has an optical transition at 5×10^{14} Hz to an excited state consisting of two hyperfine levels separated by 1 GHz. The hyperfine splitting can be determined with an uncertainty of 1 MHz if the transition frequencies to the two hyperfine levels are measured with accuracies of one part in 5×10^8. A different approach is to measure the hyperfine splitting directly, which only requires a measurement accurate to one part in 10^3. The latter task requires simpler and cheaper apparatus and is therefore in general easier.

This chapter reports on a new spectroscopic method that uses a frequency-modulated laser to excite an atomic beam. It has an especially promising future given the rapid technological advances in developing new relatively inexpensive acousto-optic and electro-optic modulators. Most significantly, this new method is free of various systematic effects that have limited the accuracy of past experiments. This chapter is organized as follows. Section II briefly reviews some of the advances made in optical spectroscopy during the last few decades. Principally, it discusses the use of Fabry–Perot etalons in conjunction with laser atomic beam spectroscopy. Interferometers have been extensively employed by numerous groups to determine many different kinds of frequency shifts. Section III describes three possible experimental arrangements using optically modulated laser beams to make frequency measurements. The advantages and limitations of these approaches are illustrated in Section IV by three specific examples of experiments that determined isotope shifts and hyperfine structure. Section V discusses some precision Stark shift measurements for optical transitions. It concludes with a summary of polarizability data having uncertainties of less than 0.5%. Sections IV and V also compare the results obtained using a variety of competing spectroscopic techniques. Finally, Section VI gives concluding remarks.

II. Optical Spectroscopy

One of the first methods developed to study spectra was to use a spectrometer to examine the light emitted by atoms excited in a discharge lamp. The width of the observed spectral lines is limited to about a gigahertz by collisional and Doppler broadening. Hence, one typically observes several overlapping lines for a transition occurring in an atom having several stable isotopes. The signals produced by the less abundant isotopes can be enhanced by loading the lamp with isotopically enriched atomic samples. An example of such an experiment was done by Ross (1963) to study the hyperfine splittings and isotope shifts of the ytterbium $(6s)^2\,{}^1S_0 \rightarrow (6s6p)\,{}^3P_1$ transition at 555.6 nm. Ytterbium has naturally occurring

isotopes with atomic mass units 168 (0.13%), 170 (3.05%), 171 (14.3%), 172 (21.9%), 173 (16.1%), 174 (31.8%), and 176 (12.7%). The nuclear spin of the even isotopes is zero, whereas isotopes 171 and 173 have spins of $\frac{1}{2}$ and $\frac{5}{2}$, respectively. The experimental resolution was further improved by cooling the lamp cathode with liquid nitrogen to reduce the Doppler width. The emitted light was filtered by a Fabry–Perot interferometer and subsequently detected with a spectrograph. The resulting hyperfine splittings and isotope shifts are listed in Table I and have uncertainties between 2 and 18 MHz.

A similar experiment was performed by Chaiko (1970) using a somewhat more sophisticated spectrometer. His results have slightly smaller uncertainties and are in good agreement with the data obtained by Ross (1963), with the single exception of the ^{173}Yb transition from the $F = \frac{5}{2}$ ground state hyperfine level to the $F = \frac{3}{2}$ hyperfine level of the excited state. The identification of this line is complicated by the very close proximity of a transition occurring in ^{171}Yb. Later, more accurate experiments have shown Chaiko's result to be in error.

A significant improvement in resolution was obtained by using narrow linewidth lasers to excite atoms in an atomic beam. This greatly reduced the collisional broadening since the atoms travel in a vacuum. The laser and atomic beams intersect orthogonally to eliminate the first order Doppler shift. This method is ideally suited for studying transitions to short-lived excited states, since lasers generate high fluxes of photons and the peak cross section for resonance scattering given by

$$\sigma_{\text{scat}} = \frac{\lambda^2}{2\pi} \tag{1}$$

is large at optical wavelengths λ. Hence, the fluorescence produced by the radiative decay of the excited state can be readily detected.

A typical experiment is illustrated in Fig. 1. An atomic beam consisting of two stable isotopes is considered. The laser frequency is scanned across the resonance while fluorescence is detected by a photomultiplier. The width of the observed spectral lines depends on various factors including the laser frequency jitter, the natural linewidth of the transition, and the laser power. Laser linewidths of 0.5 MHz are commonly achieved by commercial ring dye lasers that are electronically stabilized using an external cavity. The natural linewidth (FWHM) of a transition is given by

$$\Delta\nu_{\text{nat}} = \frac{1}{2\pi\tau} \tag{2}$$

TABLE I
ISOTOPE SHIFTS OF THE YTTERBIUM $(6s)^2\,{}^1S_0 \rightarrow (6s6p)\,{}^3P_1$ TRANSITION AT 555.6 NM

	Position relative to ^{176}Yb (MHz)					
Spectral Line	Ross (1963)	Chaiko (1970)	Broadhurst *et al.* (1974)	Clark *et al.* (1979)	Jin *et al.* (1991)	van Wijngaarden and Li (1994a)
173(5/2 → 7/2)	−1460 ± 6	−1451 ± 6	−1434.2 ± 0.6	−1431.7 ± 0.5	−1432.5 ± 4.3	−1432.6 ± 1.2
171(1/2 → 1/2)	−1187 ± 3	−1184 ± 6	−1176.1 ± 0.6	−1177.2 ± 0.5	−1176.6 ± 3.5	−1177.3 ± 1.1
176	0	0	0	0	0	0
174	947 ± 2	947 ± 2	954.6 ± 0.6	954.8 ± 0.5	953.0 ± 1.3	954.2 ± 0.9
172	1940 ± 9	1940 ± 9	1955.9 ± 0.6	1955.0 ± 0.5	1954.0 ± 2.0	1954.8 ± 1.6
170	3229 ± 18	3232 ± 6	3242.6 ± 0.6	3241.5 ± 0.5	3239.6 ± 3.2	3241.5 ± 2.8
173(5/2 → 5/2)	3247 ± 9	3253 ± 6	3267.2 ± 0.6	3266.5 ± 0.5	3264.3 ± 9.8	3267.1 ± 2.8
168	4581 ± 15		4610.6 ± 0.6	4610.1 ± 0.5	4609.5 ± 4.6	4611.9 ± 4.4
171(1/2 → 3/2)	4761 ± 9	4761 ± 9	4758.7 ± 0.6	4759.8 ± 0.5	4759.5 ± 14.3	4761.8 ± 3.7
173(5/2 → 3/2)	4749 ± 12	4700 ± 6	4764.7 ± 0.6	4760.4 ± 0.5	4759.5 ± 14.3	4761.8 ± 3.7

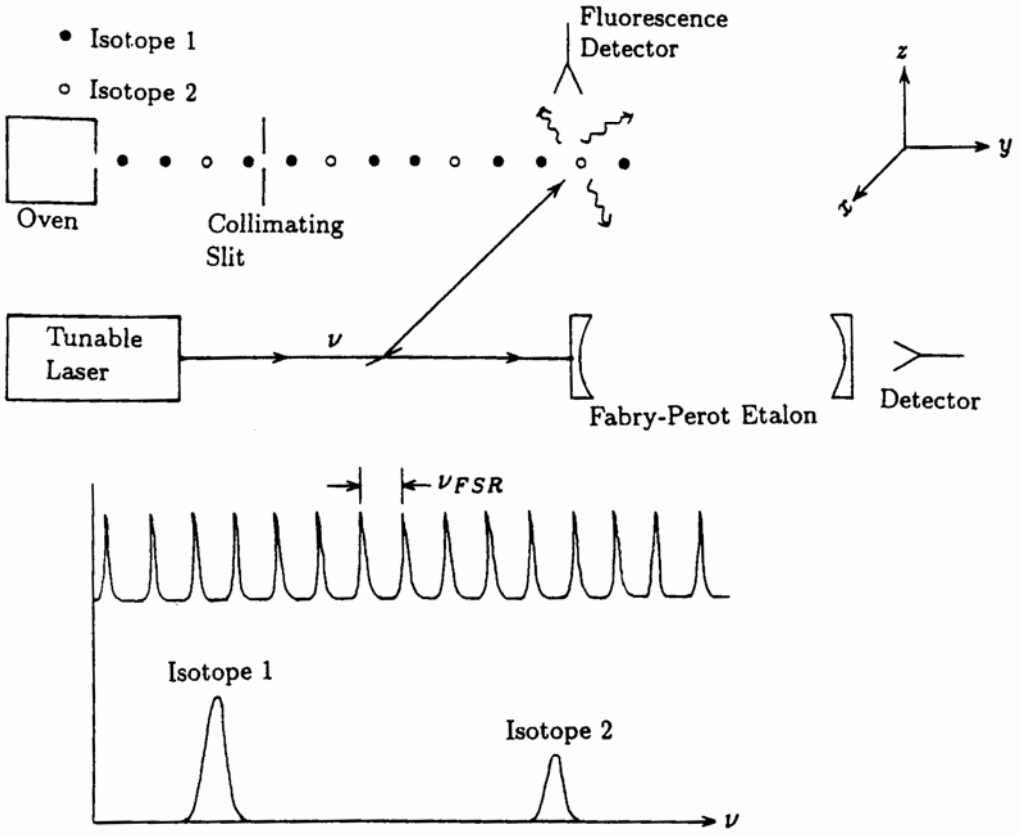

FIG. 1. Laser atomic beam spectroscopy using a Fabry–Perot etalon. See text for a detailed discussion.

where τ is the radiative lifetime of the excited state. For the ytterbium $(6s6p)^3P_1$ state, the lifetime has been found to be 8.27×10^{-7} sec (Baumann and Wandel, 1966), corresponding to a natural linewidth of 190 kHz. This is much smaller than is typical for an electric dipole allowed decay to the ground state. For example, the sodium D_1 line has a linewidth of 9.7 MHz (Carlsson *et al.*, 1992). Measurements should also be taken at low laser powers to avoid power broadening and to minimize optical pumping effects (Baird *et al.*, 1979).

The change in laser frequency is monitored by passing part of the laser beam through a Fabry–Perot etalon. The laser is transmitted through the interferometer, producing a so-called frequency marker whenever the laser frequency changes by an amount equal to the cavity's free spectral range ν_{FSR}. For a confocal etalon, the latter is given by

$$\nu_{\mathrm{FSR}} = \frac{c}{4nL} \tag{3}$$

Here, c is the speed of light, n is the index of refraction of the material (usually air) occupying the interferometer, and L is the cavity length. Hence, the etalon length must be carefully measured and be stabilized against vibrations for accurate frequency calibration. This can be done using an HeNe laser, the wavelength of which is locked to an atomic transition in iodine as is illustrated in Fig. 2. A photodetector monitors the transmission of the HeNe laser through the interferometer and feeds back a servo signal to a piezoelectric crystal on which a cavity mirror is mounted (Clark *et al.*, 1979). The mirror position is adjusted to keep the Fabry–Perot etalon locked to the laser wavelength.

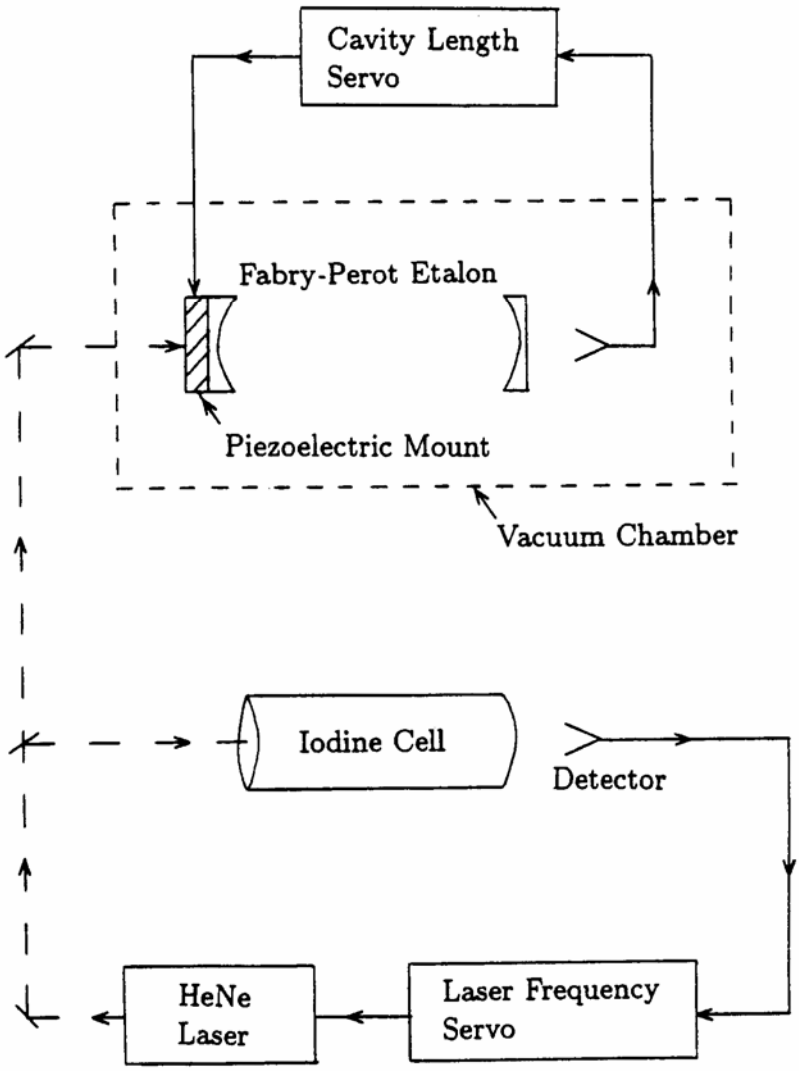

FIG. 2. Interferometer stabilization apparatus. The length of the Fabry–Perot etalon is stabilized using an HeNe laser, the wavelength of which is locked to an iodine transition.

The accuracy of the frequency determination between the frequency markers is limited by nonlinearities of the laser wavelength scan. This may be further complicated by temporal fluctuations of the laser power that affect the amplitude of the frequency markers. The calibration can be improved by decreasing the free spectral range. However, cavities with lengths in excess of two meters are impractical. Baird *et al.* (1979) attempted to resolve this problem in their study of the hyperfine structure of the barium $(6s)^2\,{}^1S_0 \rightarrow (6s6p)\,{}^1P_1$ transition by interpolating the frequency using a polynomial function to fit the marker positions. They report this permitted the determination of the laser frequency throughout the scan with an uncertainty of 0.25 MHz.

An alternative approach has been developed by Broadhurst *et al.* (1974) in their study of the ytterbium $(6s)^2\,{}^1S_0 \rightarrow (6s6p)\,{}^3P_1$ transition. The laser frequency was monitored using a confocal Fabry–Perot etalon having a free spectral range of 300.31 ± 0.02 MHz. The cavity length was stabilized to two parts in 10^{10} using an HeNe laser as is illustrated in Fig. 2. The interferometer length L therefore satisfied

$$m\lambda_{\mathrm{HeNe}} = 4nL \tag{4}$$

where m is the order of interference, $\lambda_{\mathrm{HeNe}} = 632.8$ nm, and n is the index of refraction of the air occupying the cavity. The etalon length could be changed rapidly and reproducibly corresponding to a change of the interference order to $m + 1$. This was done immediately after a transmission maxima of the dye laser was observed during a scan of the dye laser wavelength across the ytterbium resonance. Hence, the Fabry–Perot etalon acted as two cavities and generated a double set of frequency markers separated by

$$\Delta = \nu_{\mathrm{FSR}} \frac{\lambda_{\mathrm{HeNe}}}{\lambda_{\mathrm{dye}}} - 1 \tag{5}$$

For the ytterbium transition, $\lambda_{\mathrm{dye}} = 555.6$ nm and $\Delta = 41.7$ MHz. A complication was caused by air pressure fluctuations that perturbed the index of refraction differently at the dye laser and HeNe laser wavelengths. This affected the location of the frequency markers that were generated by the dye laser, whereas the cavity length was locked using the HeNe laser. The results listed in Table I (Broadhurst *et al.*, 1974) were believed to have been corrected for these effects. However, a subsequent experiment by the same group (Clark *et al.*, 1979) enclosed the interferometer in a vacuum chamber and obtained data that differed from the earlier results by as much as 4 MHz. This work also obtained improved values for the positions of the closely spaced ^{171}Yb $(F = \frac{1}{2} \rightarrow F = \frac{3}{2})$ and ^{173}Yb

($F = \frac{5}{2} \rightarrow F = \frac{3}{2}$) lines using a magnetic field of 102 G. The zero field positions of these lines were found by computing the Zeeman shifts.

Table I also lists measurements made by Jin *et al.* (1991). Their experiment is similar to that of Clark *et al.* (1979) except that their Fabry–Perot etalon only generated frequency markers every 297.7 MHz. They claim an accuracy of 0.1–0.2% for the even isotope shifts and 0.3–0.4% for the hyperfine splittings of the odd isotopes. The uncertainties listed in Table I were computed using their lower error estimates.

III. Spectroscopy Using Frequency-Modulated Lasers

A. Optical Modulators

Significant technological advances in materials during recent years have produced acousto-optic and electro-optic modulators that can frequency shift infrared, visible, and even some ultraviolet laser wavelengths. These modulators have found important uses in optical communications and in laser spectroscopy. Various articles describing the theory and applications of these devices have been written, including ones by Korpel (1988), Tran (1992), and Xu and Stroud (1992). This section focuses on making precision measurements using acousto-optic modulators. Many of the techniques presented can be readily adapted to use electro-optic modulators. Various groups have employed the latter devices to determine isotope shifts in mercury (Rayman *et al.*, 1989), helium (Zhao *et al.*, 1991), ytterbium (Deilamian *et al.*, 1993), and hydrogen (Schmidt-Kaler *et al.*, 1993).

The operation of an acousto-optic modulator is briefly summarized in Fig. 3. A modulation frequency ν_{AO} is amplified and applied to a transducer. The latter generates a pressure or sound wave inside the acousto-optic material that alters the refractive index. This produces a moving grating that diffracts portions of an incident laser beam at frequency ν. The frequencies of the outgoing laser beams are given by

$$\nu_d = \nu \pm n\nu_{\mathrm{AO}} \tag{6}$$

where n is an integer. The trajectory of the unshifted laser beam is unaffected, whereas the frequency-shifted laser beams are spatially deflected by up to a few milliradians. The amount of light diffracted into the various modes depends on the power of the modulation signal. In our experiments, a tellurium oxide crystal (Brimrose TEF 27-10) was used that had a diffraction efficiency of over 50% for shifting light at 590 nm by 220–320 MHz. The modulation signal was supplied by a computer control-

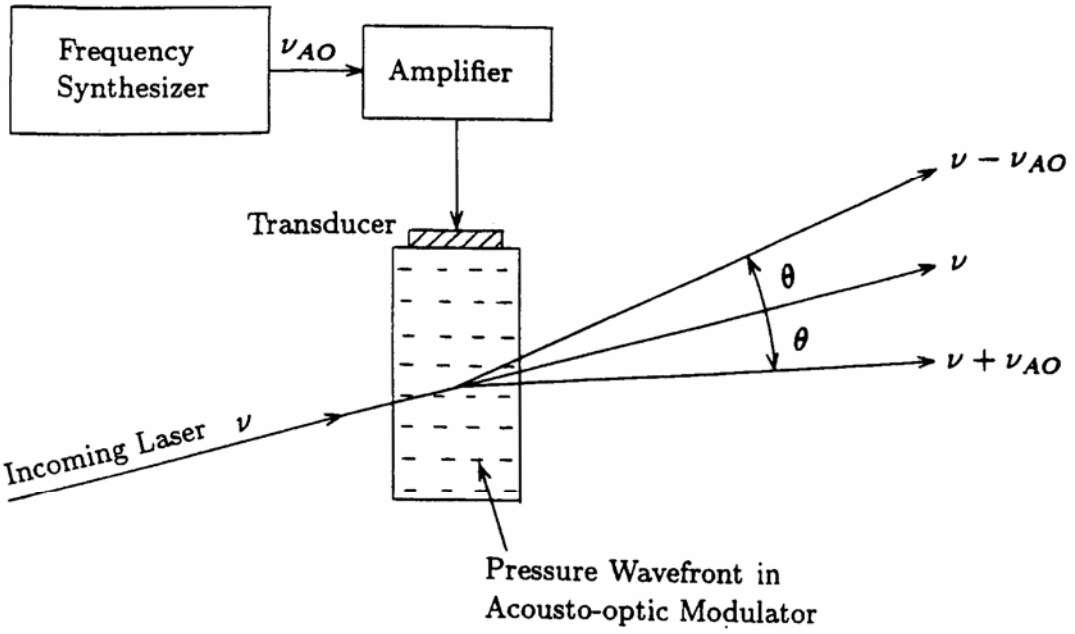

FIG. 3. Operation of an acousto-optic modulator. Part of a laser beam of frequency ν is shifted to produce diffracted beams at frequencies $\nu_d = \nu \pm n\nu_{AO}$, where n is an integer and ν_{AO} is the modulation frequency.

lable frequency synthesizer (Hewlett Packard 8645A) with an accuracy of one part per million. This signal was then amplified to a power of 1 W. Acousto-optic modulators capable of frequency shifting light up to several gigahertz are commercially available. Their operation is straightforward and the technical requirements are relatively undemanding although some units require substantial power and may therefore need to be water cooled.

B. General Experimental Arrangement

This section discusses various ways in which an acousto-optically modulated laser beam can be used to determine a frequency interval such as an isotope shift. An atomic beam is considered rather than a cell, since the fluorescent signals obtained using the latter are Doppler and collisionally broadened and therefore have inherently lower resolution. Figure 4(a) shows an atomic beam consisting of two isotopes that have transitions separated by frequency $\Delta\nu_{ISO}$. An acousto-optic modulator (AO) frequency shifts part of a laser beam at frequency ν by an amount ν_{AO}. The two laser beams at frequencies ν and $\nu - \nu_{AO}$ are superimposed and intersect the atomic beam orthogonally. Fluorescence is monitored by a detector (Det) as the laser frequency is scanned across the resonance.

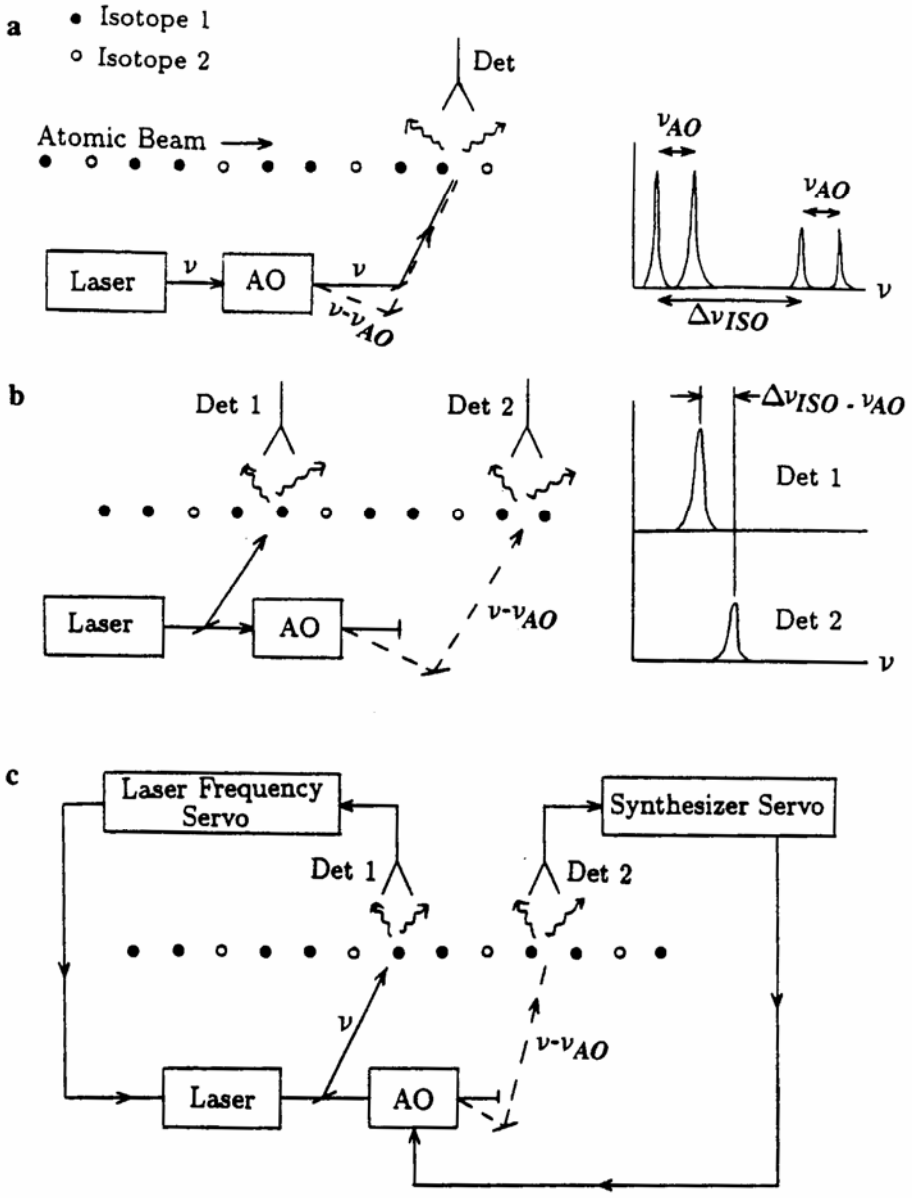

FIG. 4. Possible experimental arrangements. Details are given in the text.

Each isotope is excited once by each of the two laser beams, producing a double spectrum. The frequency axis can then be calibrated using the modulation frequency ν_{AO}, which separates each pair of peaks.

The advantage of this method is its simplicity. Only a single laser and one detector are required. It is critical however, that the frequency-shifted and unshifted laser beams be collinear. A misalignment by an angle θ produces a residual shift

$$\Delta\nu_{res} = \theta\,\Delta\nu_{Dop} \tag{7}$$

For θ equal to 1 mrad and a Doppler width of 0.5 GHz, $\Delta\nu_{res} = 0.5$ MHz. This affects the frequency calibration, since each pair of peaks in the fluorescent spectrum is then separated by $\nu_{AO} + \Delta\nu_{res}$. The laser beams can be suitably collimated using alignment slits or by passing the laser beams through a single mode optical fiber (Tanner and Wieman, 1988a). Note that this problem does not occur when using an electro-optic modulator, which generates frequency sidebands that are not spatially separated.

The accuracy of the experiment outlined in Fig. 4(a) is limited by nonlinearities of the laser frequency scan, which also affected experiments that use a Fabry–Perot etalon to calibrate the frequency as has been discussed in Section II. However, the modulation frequency applied to the optical modulator can be changed quickly and conveniently, unlike the free spectral range of an interferometer. Hence, tests can be readily made to check for the existence of scanning nonlinearities.

A second experimental setup is shown in Fig. 4(b). Two laser beams at frequencies ν and $\nu - \nu_{AO}$ intersect the atomic beam at different locations. Fluorescence is monitored by two detectors (Det 1 and Det 2) as the laser frequency is scanned across the resonance. The isotope shift is determined by finding the modulation frequency ν_{AO} such that the two isotopes are simultaneously excited by the two laser beams. This method has the advantage of being relatively insensitive to any nonlinearity of the laser scan. However, two detectors are needed, and the acousto-optic modulation frequency must match the isotope shift. The latter requirement may not be possible in the case of a large isotope shift, since the synthesizer and amplifier needed to generate modulation frequencies in excess of 2 GHz are relatively expensive.

A third option is to perform a so-called heterodyne experiment (Walther, 1974) as is shown in Fig. 4(c). The two isotopes are excited by the laser beams at frequencies ν and $\nu - \nu_{AO}$ at separate locations along the atomic beam. The signals obtained by the two detectors are used to lock the lasers to the transition frequencies. The isotope shift then equals the modulation frequency. This method has the advantage of obtaining data faster than either of the methods illustrated in Figs. 4(a) and 4(b) since the laser frequency does not need to be scanned across the resonance. It does, however, require fast electronic servo circuits that can accurately lock the laser frequency to the center of an atomic transition. A number of variations of this scheme exist. Some groups have locked two separate lasers to the different transitions (Hunter *et al.*, 1991). The frequency shift is then found by measuring the beat frequency of the two laser beams. This approach is in general only affordable when the transition can be excited using relatively inexpensive diode lasers.

The ultimate accuracy of an experiment that measures frequency shifts is limited by the natural linewidth of the transition. Very few groups have claimed the ability to determine the center of a resonance line to better than one part of a thousand of the linewidth, which for the sodium D_1 line represents only 10 kHz. A number of sometimes subtle effects including optical pumping (Holmes and Griffith, 1995), stray magnetic and electric fields, light shifts (Mathur *et al.*, 1968), second order Doppler shifts, and the presence of nearby lines (van Wijngaarden and Li, 1995) can distort the natural Lorentzian lineshape and shift the observed line center away from the transition frequency.

IV. Hyperfine Structure and Isotope Shifts

A. Background

Measurements of hyperfine structure and isotope shifts have yielded important information about nuclear structure (Arimondo *et al.*, 1977). The hyperfine Hamiltonian consists of the magnetic dipole H_{MD} and the electric quadrupole E_{EQ} terms:

$$H_{\mathrm{hyp}} = H_{\mathrm{MD}} + H_{\mathrm{EQ}} \tag{8}$$

H_{MD} describes the interaction of the nuclear magnetic moment with the magnetic field generated by the electrons. It is given by

$$H_{\mathrm{MD}} = ah\vec{I}\cdot\vec{J} \tag{9}$$

where a is called the magnetic dipole constant, h is Planck's constant, $\vec{I}$ is the nuclear spin, and $\vec{J}$ is the total electronic angular momentum. The electric quadrupole term originates from the Coulomb interaction between the electrons and a nonspherically symmetric nucleus. It is given by

$$H_{\mathrm{EQ}} = bh\left[\frac{3(\vec{I}\cdot\vec{J})^2 + (3/2)(\vec{I}\cdot\vec{J}) - \vec{I}^2\vec{J}^2}{2I(2I-1)J(2J-1)}\right] \tag{10}$$

where b is called the electric quadrupole moment coupling constant. This expression is valid only if the nuclear spin $I \geq 1$ and is zero otherwise. The eigenstates of the hyperfine Hamiltonian are designated by $|Fm_F JI\rangle$

where m_F is the azimuthal component of the angular momentum $\vec{F} = \vec{J} + \vec{I}$. The corresponding eigenenergies are

$$E_F = ah\frac{K}{2} + bh\frac{3K(K+1) - 4I(I+1)J(J+1)}{8I(2I-1)J(2J-1)} \tag{11}$$

where $K = F(F+1) - I(I+1) - J(J+1)$.

B. Ytterbium $(6s6p)\ ^3P_1$ State

An experiment similar to that outlined in Fig. 4(a) determined the hyperfine structure and isotope shifts of the ytterbium $(6s)^2\ ^1S_0 \rightarrow (6s6p)\ ^3P_1$ transition (van Wijngaarden and Li, 1994a). The apparatus is illustrated in Fig. 5. An atomic beam was generated by heating the ytterbium metal close to its melting point of 819 K. The atoms were collimated by a series of silts producing a beam having a divergence of about 1 mrad. The atomic beam traveled in a vacuum chamber that was pumped to a pressure of about 1×10^{-7} Torr using a diffusion pump.

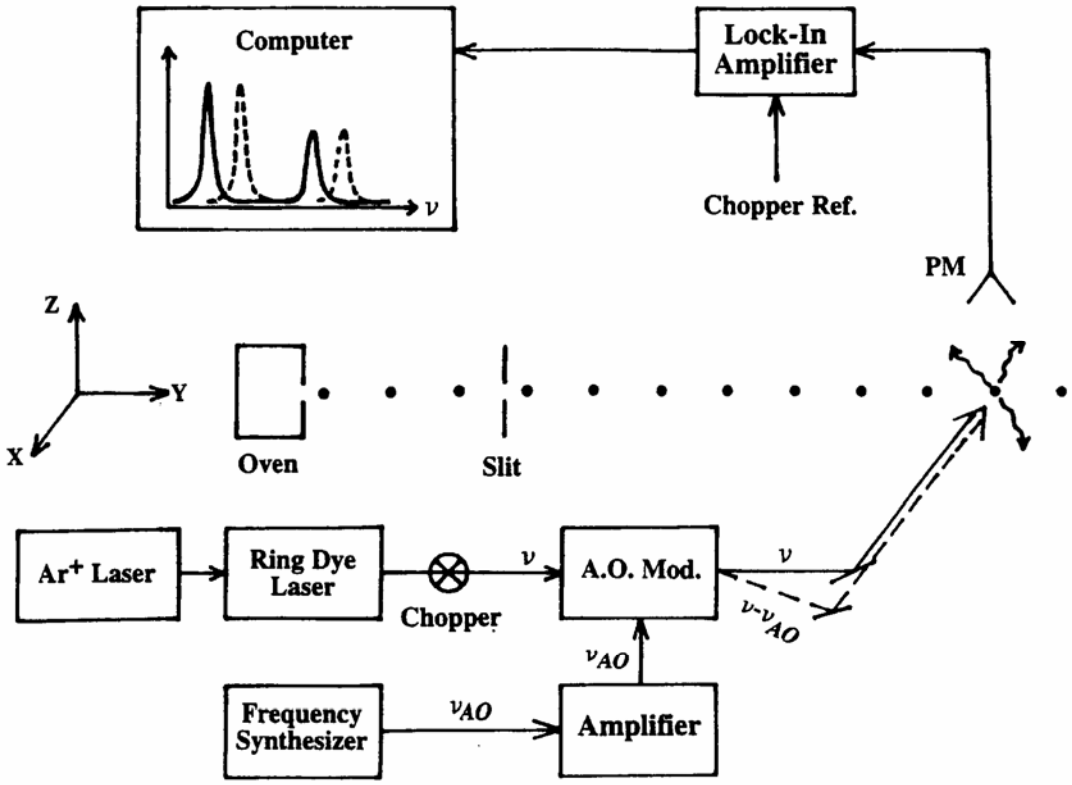

FIG. 5. Apparatus for studying hyperfine and isotope shifts of the ytterbium $(6s6p)\ ^3P_1$ state. Details are given in the text (van Wijngaarden and Li, 1994a, by permission).

The laser light was generated by a ring dye laser (Coherent 699) that was pumped by an argon ion laser. The dye laser at frequency ν was frequency shifted by an acousto-optic modulator. The frequency-shifted and unshifted laser beams were superimposed using slits placed on either side of the vacuum chamber. The two laser beams were estimated to be aligned to better than 0.3 mrad. Fluorescence was detected by a photomultiplier and recorded by a digital lock-in amplifier (Stanford Research 850). The lock-in reference signal was provided by a chopper that modulated the laser light at a frequency of about 2 kHz. The demodulated signal was digitized by the lock-in at a rate of 128 Hz. The laser was scanned across the resonance at a speed of about 50 MHz/sec. Hence, a typical 7-GHz scan shown in Fig. 6 took about 2.5 min and consisted of nearly 20,000 data points. The lock-in fitted a Gaussian function to each peak to determine the position of its line center.

The data shown in Fig. 6 were taken using an acousto-optic modulation frequency of 300.000 MHz. The laser power was attenuated to about 1 mW

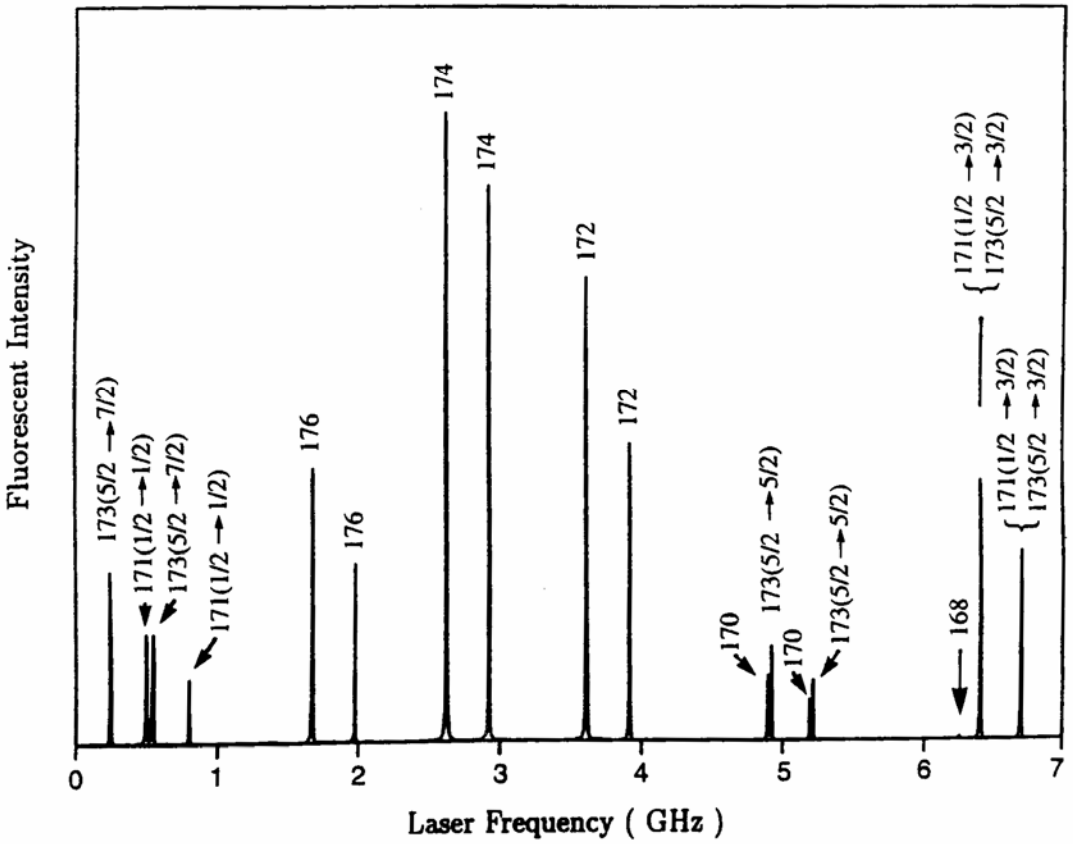

FIG. 6. Excitation of the ytterbium $(6s)^2\,{}^1S_0 \rightarrow (6s6p)\,{}^3P_1$ transition using frequency-shifted and unshifted laser beams (van Wijngaarden and Li, 1994a, by permission).

with neutral density filters to reduce the power broadening of the line. The observed linewidth (FWHM) of the spectral lines was about 7 MHz. The frequency was calibrated as follows. First, the average number of points separating the eight pairs of peaks was determined for each wavelength scan. This number was then divided into 300.000 MHz to find the frequency interval between neighboring points. The frequency calibration was affected by the laser scan speed, which varied by up to 0.1% from scan to scan. Figure 7 displays a histogram showing the number of times a particular interval separating a pair of peaks generated by the frequency-shifted and unshifted laser beams was observed. The data are fit well by a Gaussian function, as would be expected for random fluctuations of the data about an average value. It was concluded that the laser frequency

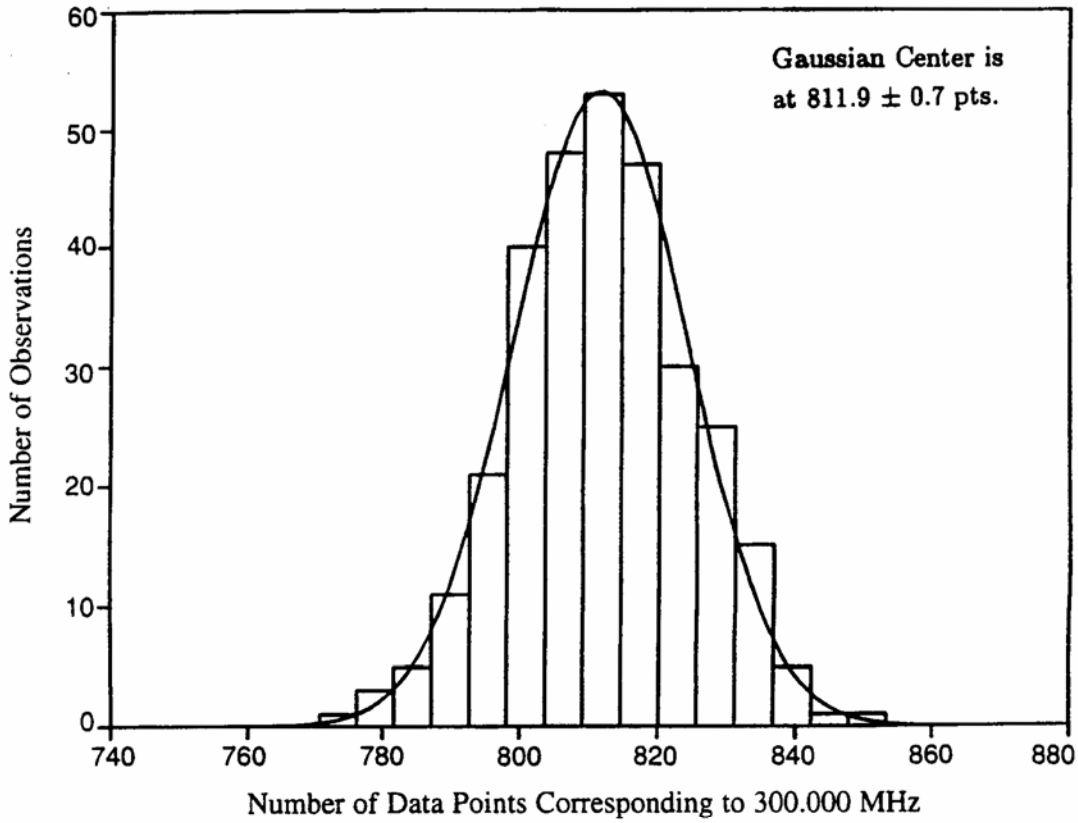

FIG. 7. Frequency calibration check of the laser scan of the ytterbium $(6s)^2\,{}^1S_0 \rightarrow (6s6p)\,{}^3P_1$ transition. The number of data points corresponding to the acousto-optic modulation frequency of 300.000 MHz was determined for 306 pairs of peaks obtained from 40 separate laser scans. The Gaussian function is centered about the average value of 811.9 ± 0.7 data points. The frequency interval between two neighboring points is therefore 0.3695 ± 0.0003 MHz (Li, 1995, by permission).

jittered randomly and that no systematic scanning nonlinearity was observed at the part in a thousand level.

The isotope shifts were obtained by averaging the data collected in 40 separate wavelength scans. The uncertainty of each result listed in Table I equals one standard deviation of the data about its average value. The results are consistent with the most accurate data obtained by Clark *et al.* (1979). The experimental accuracy is limited by the variation of the laser scan speed. The uncertainty of the isotope shifts exceed the transition's natural linewidth of 190 kHz. Hence, future experiments yielding significantly more accurate results are possible.

The hyperfine coupling constants for ^{171,173}Yb can be extracted from the data given in Table I using Eq. (11). The resulting values of the magnetic dipole and electric quadrupole coupling constants obtained by Clark *et al.* (1979) and Li (1995) are listed in Table II. The hyperfine structure has also been examined by several groups using the level crossing and optical double resonance techniques. Baumann *et al.* (1969) excited an atomic beam of ytterbium using light generated by a hollow cathode lamp. The light was directed in the x direction and was linearly polarized along the y axis. A magnet generated a field in the z direction. The field strength was measured using a proton resonance magnetometer. A photomultiplier detected fluorescence that was emitted in the y direction and linearly polarized parallel to the x axis. The magnetic field mixes the $F = \frac{1}{2}, \frac{3}{2}$ hyperfine levels of the ^{171}Yb $(6s6p)\,^3P_1$ state and also the $F = \frac{3}{2}, \frac{5}{2}, \frac{7}{2}$ hyperfine levels of the ^{173}Yb $(6s6p)\,^3P_1$ state. The fluorescence polarization changes when two levels have the same energy, which is called a level crossing. The magnetic dipole hyperfine constants were found by measur-

TABLE II
HYPERFINE CONSTANTS OF THE $(6s6p)\,^3P_1$ STATE OF ^{171}YB AND ^{173}YB

Hyperfine Constants (MHz)			
$a(^{171}\text{Yb})$	$a(^{173}\text{Yb})$	$b(^{173}\text{Yb})$	Reference
3959.1 ± 1.4	−1094.7 ± 0.6	−826.9 ± 0.9	Baumann *et al.* (1969)
3957.72 ± 0.11	−1094.35 ± 0.03	−826.59 ± 0.20	Budick and Snir (1970)
3958.23 ± 0.06	−1094.32 ± 0.04	−825.90 ± 0.09	Wandel (1970)
3957.97 ± 0.47	−1094.20 ± 0.60	−827.15 ± 0.47	Clark *et al.* (1979)
3959.1 ± 3.0	−1094.44 ± 0.84	−827.89 ± 0.85	Li (1995)

ing the magnetic fields H_c at which the level crossings occurred and using the relations

$$a(^{171}\mathrm{Yb}) = 0.99987 g_J \frac{\mu_B}{h} H_c(^{171}\mathrm{Yb}) \tag{12}$$

$$a(^{173}\mathrm{Yb}) = -0.33705 g_J \frac{\mu_B}{h} H_c(^{173}\mathrm{Yb}) \tag{13}$$

Here, μ_B is the Bohr magneton and g_J is the gyromagnetic factor. The latter quantity was determined in an optical double resonance experiment (Baumann and Wandel, 1968) that selectively populated the $m_J = 0$ Zeeman sublevel of the $(6s6p)^3P_1$ state using light polarized parallel to the magnetic field. A radio frequency field was then applied that transferred some of the atoms to the $m_J = \pm 1$ sublevels of the excited state. The gyromagnetic factor was determined by measuring the radio-frequency and the corresponding magnetic field strength. The result of 1.49285 ± 0.00005 for g_J is in excellent agreement with the value 1.49280 ± 0.00004 that was obtained in a nearly identical experiment (Budick and Snir, 1967). Baumann *et al.* (1969) determined the electric quadrupole constant $b(^{173}\mathrm{Yb})$ using an optical double resonance experiment that measured the energy separating the $F = \frac{3}{2}$ and $F = \frac{5}{2}$ hyperfine levels of the $(6s6p)^3P_1$ state at zero magnetic field.

An improved level crossing experiment has been done by Budick and Snir (1970). The size of the fluorescent signal was increased by loading isotopically enriched ytterbium in the atomic beam oven. In addition, a more homogeneous magnetic field claimed to be uniform to one part in 10^5 over a volume of 1 in.^{3} was used. This reduced the linewidth of the level crossing signals to 0.14 G, which is close to the limit set by the natural linewidth.

The hyperfine coupling constants have also been determined by Wandel (1970) using an optical double resonance experiment that measured the splittings between the various hyperfine levels of the $(6s6p)^3P_1$ state at zero magnetic field. His results shown in Table II claim a slightly improved accuracy compared with those obtained by Budick and Snir (1970). It is disturbing however, that the results obtained by these two experiments for $a(^{171}\mathrm{Yb})$ and $b(^{173}\mathrm{Yb})$ disagree. The differences of about 0.5 MHz correspond to the uncertainty obtained in the experiment of Clark *et al.* (1979) that measured the frequency shifts using an optical spectroscopic method. Hence, an improved measurement such as outlined in Fig. 4(b) or 4(c)

would be useful to help resolve the discrepancy between the data obtained by the level crossing and optical double resonance techniques.

C. Sodium $3P_{1/2}$ State

The hyperfine structure of the sodium $3P_{1/2}$ state has been intensively studied by many researchers using a variety of spectroscopic methods. A recent experiment (van Wijngaarden and Li, 1994b) scanned a laser across the D_1 line while fluorescence produced by the radiative decay of the $3P_{1/2}$ state was detected. This line consists of four transitions between the $F = 1$ and $F = 2$ hyperfine levels of the $3S_{1/2}$ and $3P_{1/2}$ states as is illustrated in Fig. 8. A sample fluorescence signal is shown in Fig. 9. The frequency scan was calibrated using the ground state hyperfine splitting, which separates the first and third peaks as well as the second and fourth peaks appearing in the spectrum. The splitting between the hyperfine

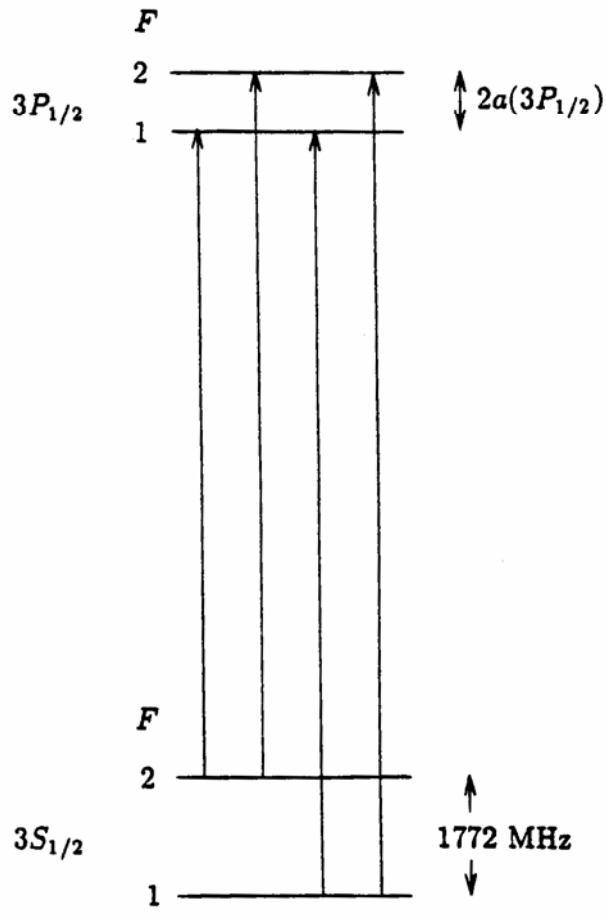

Fig. 8. Hyperfine levels of the sodium $3S_{1/2}$ and $3P_{1/2}$ states.

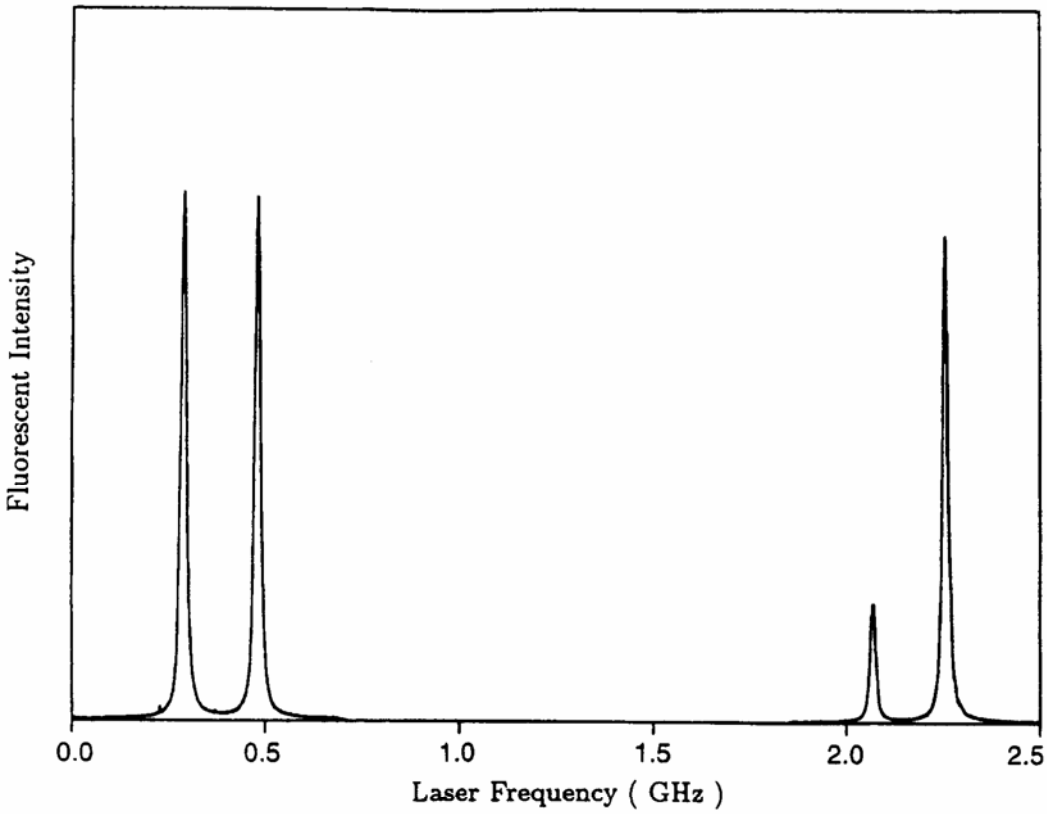

FIG. 9. Laser excitation of the sodium D_1 line. These data were taken using an apparatus similar to that shown in Fig. 5. Neutral density filters attenuated the laser power to reduce the power broadening of the line. The spectral linewidth was observed to be 12 MHz (FWHM), which compares with the natural linewidth of 9.7 MHz (van Wijngaarden and Li, 1994b, by permission).

levels of the $3S_{1/2}$ state has been determined using Ramsey's method of separated oscillatory fields (Ramsey, 1956) to be $1771.626129 \pm (1 \times 10^{-6})$ MHz (Beckmann *et al.*, 1974). This result is significantly more accurate than any frequency generated by a commercial synthesizer, and therefore an acousto-optically modulated laser beam was not used to calibrate the laser scan. The experiment was, however, similar to that illustrated in Fig. 4(a) and therefore potentially suffered from similar systematic effects including scanning nonlinearities of the laser frequency. The resulting value of 94.44 ± 0.13 MHz for the magnetic dipole hyperfine constant of the $3P_{1/2}$ state was found by averaging data produced by 200 separate wavelength scans. The uncertainty represents one standard deviation of the data about the average value. A comparison of this result with data found using other spectroscopic techniques therefore provides a strong test

TABLE III
MAGNETIC DIPOLE HYPERFINE CONSTANT OF THE SODIUM $3P_{1/2}$ STATE

a (MHz)	Method	Reference
94.45 ± 0.50	Atomic Beam Magnetic Resonance	Perl *et al.* (1955)
94.3 ± 0.2	Optical Double Resonance	Hartmann (1970)
94.25 ± 0.15	Saturation Spectroscopy	Pescht *et al.* (1977)
94.465 ± 0.010	Optical Heterodyne	Griffith *et al.* (1977)
94.42 ± 0.19	Quantum Beat Spectroscopy	Carlsson *et al.* (1992)
94.05 ± 0.20	Fabry–Perot Spectroscopy	Windholtz *et al.* (1992)
94.44 ± 0.13	Modulated Laser Spectroscopy	van Wijngaarden and Li (1994b)
94.4065 ± 0.0015	Optical Heterodyne	Young and Griffith (1994)
91.7	Many-Body Perturbation Theory	Lindgren *et al.* (1976)
91.40	Many-Body Perturbation Theory	Johnson *et al.* (1987)
93.02	Many-Body Perturbation Theory	Salomonson and Ynnerman (1991)
88.56	Multiconfiguration Hartree–Fock Theory	Carlsson *et al.* (1992)

of the validity of using modulated laser beams to measure frequency intervals.

Table III lists the most accurate data found in the literature for the magnetic dipole hyperfine constant of the $3P_{1/2}$ state. Perl *et al.* (1955) used the so-called atomic beam magnetic resonance method. A beam of sodium atoms was passed through three successive regions, A, B, and C. Atoms occupying the $m_J = -\frac{1}{2}$ ground state Zeeman sublevel were deflected out of the beam in region A by an inhomogeneous magnetic field and subsequently blocked by a beam stop. In the intermediate region B, light generated by a lamp excited some of the atoms to the $3P_{1/2}$ state in the presence of a uniform magnetic field. A radiofrequency field was also applied, which induced transitions among the levels of the excited state. Some of the atoms decayed to the $m_J = -\frac{1}{2}$ ground state Zeeman sublevel and were focused onto a hot wire detector in region C by an inhomogeneous magnetic field. The beam intensity was then monitored as

a function of the radiofrequency. This experiment is analogous to an optical double resonance experiment where a change of the beam intensity corresponds to a change of the fluorescent polarization. The accuracy was limited by various effects including a relatively poor signal to noise ratio as compared with later experiments that monitored fluorescence generated by using lasers to excite the $3P_{1/2}$ state.

Hartmann (1970) studied the $3P_{1/2}$ state using an optical double resonance experiment. A lamp excited sodium atoms contained in a vapor cell. The atoms were subjected to magnetic fields of up to 5000 G that were measured using a proton resonance magnetometer. The field was uniform to one part in 10^4. The hyperfine coupling constant was determined by measuring the radiofrequency needed to induce a transition between the levels of the excited $3P_{1/2}$ state. The experiment also obtained a value for the gyromagnetic ratio $g_J(3P_{1/2}) = 0.66581 \pm 0.00012$, which agrees well with the result of 0.66589 calculated using the Landé formula (Corney, 1977).

A saturation spectroscopy experiment has been done by Pescht *et al.* (1977). Two laser beams originating from the same dye laser were incident on a sodium cell. One laser beam saturated the $3S_{1/2} \rightarrow 3P_{1/2}$ transition while the transmission of the second so-called probe laser through the cell was measured. The dye laser was tuned across the D_1 resonance, and a reduction in the absorption of the probe laser occurred whenever the first laser excited a hyperfine level of the $3P_{1/2}$ state. The change in laser wavelength was initially monitored using a Fabry–Perot etalon having a free spectral range of 150 MHz. This permitted the hyperfine splitting of the $3P_{1/2}$ state to be determined with an uncertainty of a few megahertz. The experimental accuracy was limited by temperature fluctuations that affected the interferometer's optical length. An improved frequency calibration was performed using two HeNe lasers. The dye laser was locked to the Fabry–Perot cavity, which in turn was locked to a free running HeNe laser. This HeNe laser was frequency offset from a second HeNe laser, the frequency of which was lamp-dip stabilized to ± 50 kHz. The dye laser was then tuned by varying the frequency offset of the two HeNe lasers, which was measured using a frequency counter.

Griffith *et al.* (1977) used an optical heterodyne experiment to measure the hyperfine structure. Two separate dye lasers were superimposed and excited an atomic beam at the same location. Fluorescence was detected by a single photomultiplier. The resulting signal was used to lock the two separate lasers to the $3S_{1/2}(F = 2) \rightarrow 3P_{1/2}(F = 1)$ and the $3S_{1/2}(F = 2) \rightarrow 3P_{1/2}(F = 2)$ transition frequencies, respectively. Portions of the two laser beams were then focused onto a fast photodiode, which measured the

beat frequency. The magnetic dipole constant of the $3P_{1/2}$ state was found to be 94.46 ± 0.01 MHz. This uncertainty is impressive since the authors mention that an angular separation of only 0.1 mrad between the two laser beams would produce an error of 0.1 MHz. This effect should reverse when the lasers are interchanged between the two transitions. Hence, the final value for the magnetic dipole constant is the average of equal numbers of beat frequency readings obtained with the first laser exciting initially the $F = 1$ the later the $F = 2$ hyperfine levels of the $3P_{1/2}$ state. A recent conference proceeding (Young and Griffith, 1994) by the same group reports a value of 94.4065 ± 0.0015 MHz for $a(3P_{1/2})$. The ground state hyperfine splitting was also measured and found to be within a few kilohertz of the accepted value found using Ramsey's method of oscillatory magnetic fields. This improved version of their earlier work used the saturated absorption signal observed in a sodium vapor cell to lock the frequency of one laser while the second laser excited an atomic beam. The 1.5 kHz claimed uncertainty is less than one part in 5000 of the natural linewidth of the sodium D_1 line. Unfortunately, no reason is given to explain why the results of their two experiments disagree by more than five times the standard deviation given in their earlier work. It is hoped that a more detailed account of their experiment will soon be published.

Carlsson *et al.* (1992) studied the hyperfine structure using quantum beat spectroscopy. A mode-locked dye laser produced 6-psec pulses at a repetition rate of a few megahertz. The laser excited an atomic beam, producing an excited state that was a superposition of the hyperfine levels of the $3P_{1/2}$ state. The resulting temporal oscillations of the fluorescent intensity decay curve were measured using photon counting. The laser pulse was detected by a photodiode, whereas the fluorescence was monitored by a Peltier-cooled microchannel plate photomultiplier tube. The time difference of these two signals was measured with a time to amplitude converter (TAC). The high signal to noise ratio of their data was demonstrated by a sample fluorescent decay curve that displays nearly 25 clearly visible temporal oscillations. Values of 94.363 ± 0.054 and 94.485 ± 0.031 MHz were found for the magnetic dipole hyperfine constant $a(3P_{1/2})$ using TAC settings of 200 and 500 nsec, respectively. These two results were averaged and the 0.15% uncertainty of the time scale was included to give 94.42 ± 0.19 MHz. The experiment was checked by determining the radiative lifetime of the $3P_{1/2}$ state. A value of 16.35 ± 0.06 nsec was obtained, which agrees very well with 16.38 ± 0.08 nsec found previously by Carlsson (1988) using the same technique. Two other experiments using the so-called fast beam laser technique have obtained values of 16.40 ± 0.03 (Gaupp *et al.*, 1982) and 16.40 ± 0.05 nsec (Schmoranzer *et al.*, 1979).

It should be noted that these data are among the most accurate lifetimes published in the literature.

Umfer *et al.* (1992) studied the effects on the sodium D_1 line of magnetic fields of up to 10,000 G. A ring dye laser excited a sodium atomic beam. Spectra were obtained by scanning the laser frequency across the D_1 line and observing the fluorescence detected by a photomultiplier. The laser scan was calibrated by passing a portion of the laser beam through an etalon having a free spectral range of 197.5974 $\pm$ 0.0003 MHz. The fluorescent peaks had a linewidth (FWHM) of 16 MHz. The magnetic field was determined using a nuclear magnetic resonance gaussmeter with an accuracy of better than 0.1 G. The magnetic field mixes the hyperfine levels of the excited state and thereby changes the various transition frequencies making up the D_1 line. An analysis of the spectra determined $a(3P_{1/2})$ to be 94.05 $\pm$ 0.20 MHz.

Table III lists the values found for the magnetic dipole hyperfine constant of the sodium $3P_{1/2}$ state by seven independent research groups, which each used a different measurement technique. All the data are in agreement except the two conflicting results obtained by the group of Griffiths *et al.* This supports the validity of the experimental method used by van Wijngaarden and Li (1994b), which is closely analogous to that shown in Fig. 4(a). The theoretical estimates are in poor agreement with the measured values. Three independent many-body perturbation theory calculations have yielded values of 91.7 (Lindgren *et al.*, 1976) 91.40 (Johnson *et al.*, 1987), and 93.02 MHz (Salomonson and Ynnerman, 1991) for $a(3P_{1/2})$. Carlsson *et al.* (1992) used wavefunctions found using a multiconfiguration Hartree–Fock computer code to obtain a value of 88.56 MHz. The discrepancy between theory and experiment indicates the need for improved theoretical models of many-body systems such as the sodium atom.

D. Cesium $6P_{3/2}$ State

A measurement of the hyperfine structure of the cesium $6P_{3/2}$ state has been made by Tanner and Wieman (1988b) using the approach outlined in Fig. 4(b). Their apparatus is shown in Fig. 10. Light at 852 nm corresponding to the $6S_{1/2} \rightarrow 6P_{3/2}$ transition in cesium was generated by a diode laser. The linewidth of the latter was reduced to about 20 kHz by passively locking the laser to a Fabry–Perot etalon external to the laser. Part of the laser beam was sent into a saturation spectrometer. The resulting signal was used to lock the external cavity so that the laser excited one of the hyperfine levels of the $6P_{3/2}$ state. The remaining portion of the laser beam was frequency shifted by an acousto-optic modulator. The

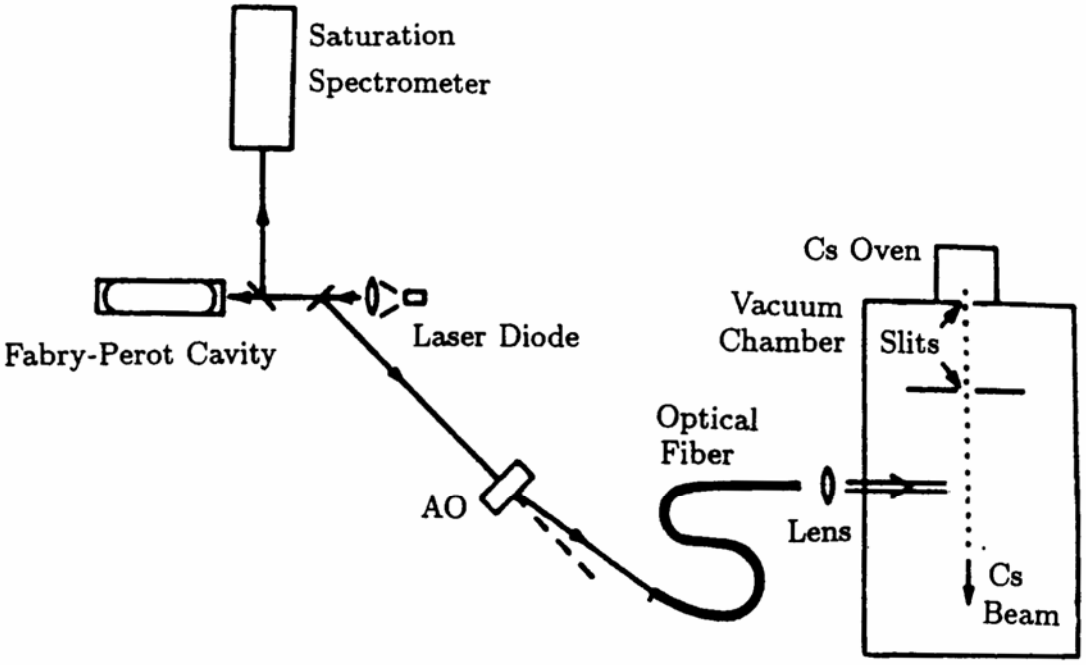

FIG. 10. Apparatus for studying the hyperfine structure of the cesium $6P_{3/2}$ state. Details are given in the text (adapted from Tanner and Wieman, 1988a, by permission).

frequency-shifted beam passes through an optical fiber and intersected the atomic beam orthogonally. Fluorescence was detected by a cooled silicon photodiode. The acousto-optic modulation frequency was adjusted to bring the light into resonance with the various hyperfine levels of the $6P_{3/2}$ state. Data were taken using a laser intensity of 13 $\mu W/cm^2$ to reduce optical pumping effects, which can shift the resonance in the presence of stray magnetic fields. The results obtained for the hyperfine level splittings are given in Fig. 11, and the magnetic dipole and electric quadrupole hyperfine constants are listed in Table IV. The measurement precision was limited by the drift of the locked laser frequency.

Table IV also lists data obtained by several other groups. The hyperfine structure of the cesium $6P_{3/2}$ state was first studied by Buck *et al.* (1956). The method and apparatus were identical to that used to study the sodium $3P_{1/2}$ hyperfine structure, which has been discussed in Section IV.C (Perl *et al.*, 1955). A computational mistake in their paper was discovered by Violino (1969). Table IV lists the corrected values for the hyperfine constants.

Three level crossing experiments have also examined the $6P_{3/2}$ state (Kallas *et al.*, 1965; Violino, 1969; Svanberg and Rydberg, 1969). All of them used light generated by a lamp to excite cesium atoms in a cell. The results of Kallas *et al.* (1965) disagree with theory according to Arimondo

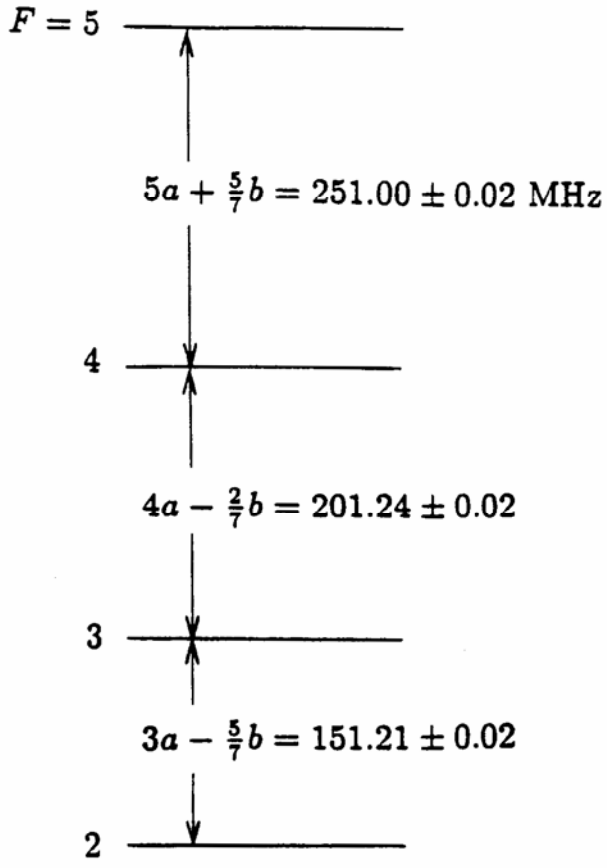

FIG. 11. Measured hyperfine splittings of the cesium $6P_{3/2}$ state (Tanner and Wieman, 1988b, by permission).

et al. (1977), leading them to conclude that the error was underestimated. Svanberg and Rydberg (1969) analyzed their data using a value for the gyromagnetic ratio of 1.345 that disagrees with the theoretical value of 1.3341 as well as a subsequent experimental measurement of 1.3340 ± 0.0003 (Abele, 1975). Their experiment yields a value of $a(6P_{3/2}) = 50.31 \pm 0.04$ MHz when the corrected value for g_J is used.

Two optical double resonance experiments have also been done. The experiments were similar to that carried out in sodium by Hartmann (1970), which has been described in Section IV.C. Svanberg and Belin (1972) determined the frequency for transitions between hyperfine levels of the $6P_{3/2}$ state in a zero magnetic field. The data was extrapolated to zero radiofrequency power. The experiment of Abele (1975) was done using a magnetic field of 1300 G.

Data obtained by the various experiments are in reasonable agreement. However, the data of Tanner and Wieman (1988b) are 10 times more precise than that of the previous best measurement. The experimental

TABLE IV
HYPERFINE CONSTANTS OF THE CESIUM $6P_{3/2}$ STATE

a (MHz)	b (MHz)	Method	Reference
50.67 ± 0.11	−0.46 ± 0.53	Atomic Beam Magnetic Resonance	Buck *et al.* (1956)
50.9 ± 0.5	−0.9 ± 0.6	Level Crossing	Kallas *et al.* (1965)
50.45 ± 0.08	−0.66 ± 0.72	Level Crossing	Violino (1969)
50.72 ± 0.03	−0.38 ± 0.18	Level Crossing	Svanberg and Rydberg (1969)
50.31 ± 0.05	−0.30 ± 0.33	Optical Double Resonance	Svanberg and Belin (1972)
50.02 ± 0.25		Optical Double Resonance	Abele (1975)
50.275 ± 0.003	−0.53 ± 0.02	Modulated Laser Spectroscopy	Tanner and Wieman (1988b)
49.785		Many-Body Perturbation Theory	Blundell *et al.* (1991)

results are substantially more accurate than a many-body perturbation theory computation (Blundell *et al.*, 1991), as was also found to be the case for the sodium $3P_{1/2}$ state.

V. Stark Shifts

A. BACKGROUND

Precise measurements of Stark shifts provide information about polarizabilities of atomic states that are important for describing a number of properties including charge-exchange cross sections, van der Waals constants, and dielectric constants (Bonin and Kadar-Kallen, 1993). Some of the first determinations of polarizabilities were made by measuring the deflection of an atomic beam as it passed through an inhomogeneous electric field (Chamberlain and Zorn, 1963). These experiments yielded results that had a typical accuracy of about 10%. Improved data was obtained by the Bederson group using both inhomogeneous magnetic and electric fields. An atomic beam is not deflected if the forces exerted by inhomogeneous magnetic H and electric fields E cancel, i.e., $\alpha E\, dE/dz = \mu\, dH/dz$. The polarizability can then be found provided the field gradients and the magnetic dipole moment μ are known. This technique has yielded results with uncertainties of a few percent (Molof *et al.*, 1974). Recently, several new methods have been developed. The ground state polarizabilities of rubidium (Bonin and Kadar-Kallen, 1993) and uranium (Kadar-

Kallen and Bonin, 1994) have been determined to 10% accuracy by measuring the deflection of an atomic beam as it passed through a standing wave generated using a Nd:YAG laser pulse. A significant improvement in accuracy has been obtained by Ekström *et al.* (1995) using atom interferometric methods. They determined the sodium ground state polarizability with an uncertainty of 0.3%. Various other methods to determine polarizabilities exist, and the reader is referred to the review articles written by Miller and Bederson (1977, 1988).

The Stark shifts of a number of transitions have recently been measured with uncertainties as low as a few parts in 10^4. This accuracy is substantially better than that attained in the best lifetime measurements (Rafac *et al.*, 1994) and by experiments that determine transition oscillator strengths (van Wijngaarden *et al.*, 1986). These data therefore permit stringent tests of atomic theory. Accurate theoretical models of many-electron atoms are especially important for improved tests of parity violation in atoms such as cesium (Hoffnagle *et al.*, 1981; Noecker *et al.*, 1988; Dzuba *et al.*, 1989; Bouchiat, 1991; Blundell *et al.*, 1991). A similar experiment has recently been proposed for ytterbium (DeMille, 1995). A thorough understanding of Stark shifts is also needed for experiments searching for an electron dipole moment (Hunter *et al.*, 1988). Accurate Stark shift data are also desired for applications such as the measurement of electrode spacings (Neureiter *et al.*, 1986) and the determination of electric fields in plasmas (Lawler and Doughty, 1995; Rebhan *et al.*, 1981). An electric field can then be found by measuring the frequency shift of a spectral line. This has a significant advantage over methods that measure fields using invasive probe electrodes which can strongly perturb the plasma.

The Hamiltonian describing the interaction of an atoms with an external electric field E is given by (Khadjavi *et al.*, 1968)

$$H_{\text{Stark}} = -\left[\alpha_0 + \alpha_2 \frac{3J_z^2 - \vec{J}^2}{J(2J-1)}\right]\frac{E^2}{2} \tag{14}$$

where $\vec{J}$ is the electronic angular momentum and the quantization axis z lies along the field direction. For $J < 1$, the second term vanishes. The terms α_0 and α_2 are the scalar and tensor polarizabilities, respectively, and are defined by

$$\alpha_0 = \frac{r_0}{4\pi^2} \sum_{j'} \lambda_{JJ'}^2 f_{JJ'} \tag{15}$$

$$\alpha_2 = \frac{r_0}{8\pi^2} \frac{1}{(2J+3)(J+1)} \sum_{J'} \lambda_{JJ'}^2 f_{JJ'} [8J(J+1) - 3X(X+1)] \tag{16}$$

where $X = J'(J' + 1) - 2 - J(J + 1)$. Here, r_0 is the classical electron radius, $\lambda_{JJ'}$ is the wavelength for a transition between states J and J', and $f_{JJ'}$ is the transition oscillator strength. The eigenstates of the Stark Hamiltonian are $|Jm_J\rangle$, where m_J is the azimuthal quantum number. The corresponding eigenenergy is

$$E_{Jm_J} = -\left[\alpha_0 + \alpha_2 \frac{3m_J^2 - J(J+1)}{J(2J-1)}\right]\frac{E^2}{2} \tag{17}$$

The eigenenergy corresponding to a hyperfine level $|Fm_F\rangle$ is given by Eq. (17) with J and m_J replaced by F and m_F, respectively.

B. Ytterbium $(6s)^2\ {}^1S_0 \rightarrow (6s6p)\ {}^3P_1$ Transition

The Stark shift of the ytterbium $(6s)^2\,{}^1S_0 \rightarrow (6s6p)\,{}^3P_1$ transition has been studied using the method outlined in Fig. 4(a) (Li and van Wijngaarden, 1995b). The apparatus shown in Fig. 12 was also used to study the Stark

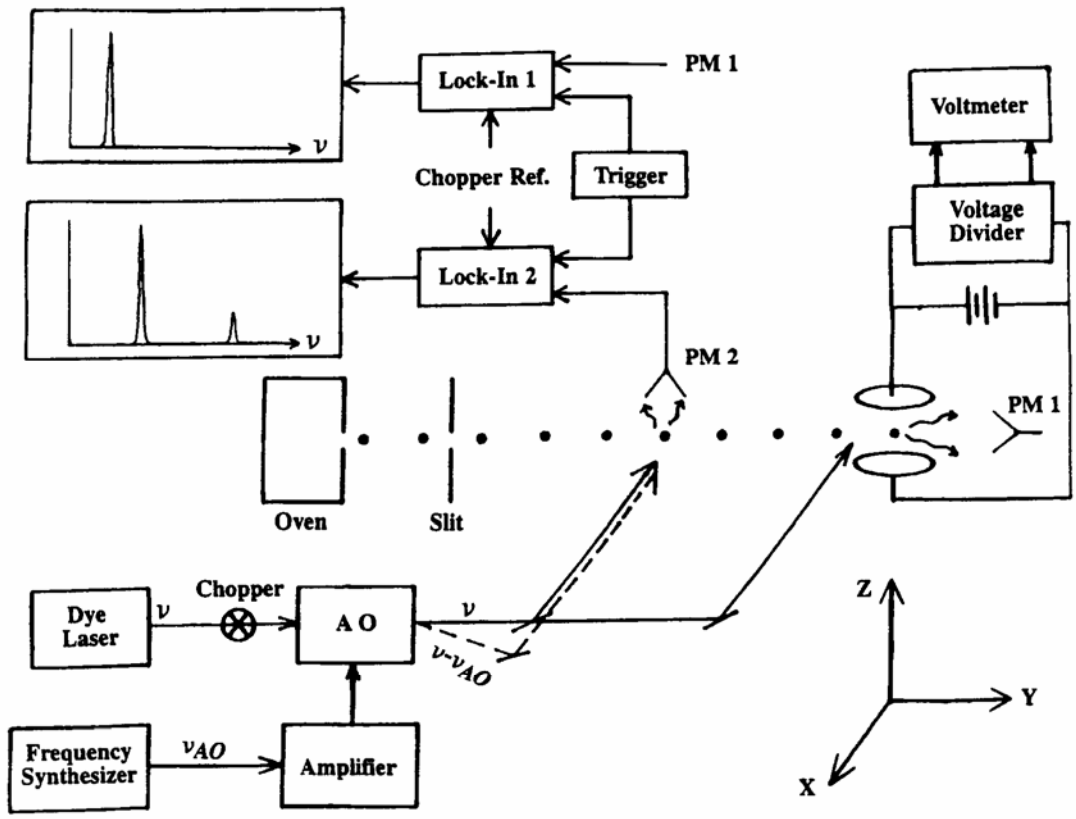

FIG. 12. Stark shift measurement apparatus. Details are given in the text (Li and van Wijngaarden, 1996, by permission).

shifts of transitions in barium (Li and van Wijngaarden, 1995a) and calcium (Li and van Wijngaarden, 1996). The generation of an atomic beam and the fluorescent detection has been discussed in Section IV.B. Ytterbium atoms were excited by a laser in a field-free region and in a uniform electric field. The electric field was generated using two highly polished stainless steel disks having a diameter of 7.62 cm. The spacing was determined to be 1.0163 ± 0.0003 cm using precision machinist blocks, the size of which was specified to within 2.5×10^{-5} cm. Plate voltages of up to 50 kV were continuously monitored using a precision voltage divider that reduced the voltage by a factor of 5000 with an accuracy of 0.01% (Julie Labs KV-50/01). The reduced voltage was measured by a voltmeter with an uncertainty of less than 0.002%.

The electric field shifts the transition by an amount

$$\Delta\nu = KE^2 \tag{18}$$

where the Stark shift rate

$$K = -\tfrac{1}{2}\left\{\alpha_0\left({}^3P_1\right) - 2\alpha_2\left({}^3P_1\right) - \alpha_0\left({}^1S_0\right)\right\} \tag{19}$$

Here, m_J has been set to zero since the laser was linearly polarized along the quantization axis, which was specified by the electric field. Hence, only the $m_J = 0$ sublevel of the $(6s6p)\,{}^3P_1$ state was populated. Equation (19) holds for the even isotopes of ytterbium that do not have a nuclear spin. For ^{171,173}Yb, the hyperfine interaction must also be considered. For simplicity, only the transition in ^{171}Yb to the $F = \frac{1}{2}$ level of the $(6s6p)\,{}^3P_1$ state was studied, which has a Stark shift rate given by

$$K\left({}^{171}\mathrm{Yb}, F = \tfrac{1}{2}\right) = -\tfrac{1}{2}\left\{\alpha_0\left({}^3P_1\right) - \alpha_0\left({}^1S_0\right)\right\} \tag{20}$$

The tensor polarizability of the $^3P_1$ state could then be determined by subtracting (20) from (19). The laser frequency was tuned across the transition while fluorescence produced by the radiative decay of the excited state to the ground state was detected by two photomultipliers (PM1 and PM2). The signals were processed by separate lock-in amplifiers. Spectra similar to that shown in Fig. 6 were obtained, and the frequency was calibrated as has been described in Section IV.B.

The results of nearly 500 wavelength scans taken at various electric fields are shown in Fig. 13. A least squares fit of a straight line $y = KE^2 + y_0$ to the data yielded $K = -15.419 \pm 0.048$ kHz/(kV/cm)^2. The frequency shift at zero field y_0 was 5.33 MHz. This offset arises from a small difference of the intersection angle of the laser and atomic beams in the field and field-free regions. The tensor polarizability was found to be $\alpha_2 = 5.81 \pm 0.13$ kHz/(kV/cm)^2. The result is in good agreement with

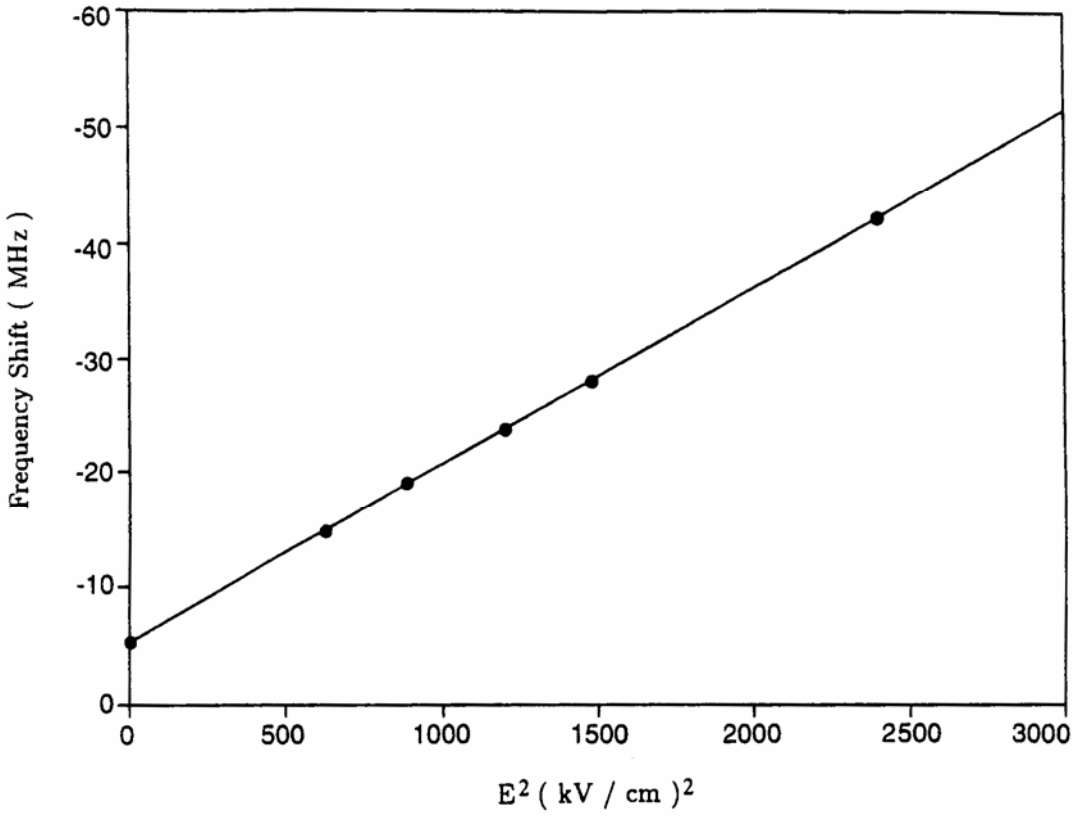

FIG. 13. Frequency shift versus electric field squared for the ytterbium $(6s)^2\,{}^1S_0 \rightarrow (6s6p)\,{}^3P_1$ transition (Li and van Wijngaarden, 1995b, by permission).

5.99 ± 0.34 kHz/(kV/cm)^2 found by an optical double resonance experiment (Rinkleff, 1980) and 6.04 ± 0.21 kHz/(kV/cm)^2 obtained using quantum beat spectroscopy (Kulina and Rinkleff, 1982).

C. CESIUM $6P_{3/2} \rightarrow nS_{1/2}$ ($n = 10$–13) TRANSITIONS

An example of a Stark shift measured as illustrated in Fig. 4(b) is an experiment that studied the $6P_{3/2} \rightarrow (10\text{–}13)S_{1/2}$ transitions in cesium (van Wijngaarden *et al.*, 1994). The apparatus was similar to that shown in Fig. 12. An oven generated two cesium atomic beams propagating in opposite directions. One atomic beam passed through a field-free region, whereas the other beam traveled through a uniform electric field. Atoms were excited from the $6S_{1/2}$ ground state to the $6P_{3/2}$ state by a diode laser that generated a few milliwatts of light at 852 nm. A ring dye laser then excited the $6P_{3/2} \rightarrow nS_{1/2}$ ($n = 10$–13) transition. Part of the dye laser was frequency shifted by an acousto-optic modulator. The unshifted laser beam at frequency ν excited the atoms in the field-free region,

whereas the laser beam having frequency $\nu - \nu_{AO}$ excited the atoms passing through the electric field. Fluorescence from the field and field-free regions was recorded as the dye laser frequency ν was scanned across the resonance. The frequency interval separating the fluorescent peak observed in the two regions was given by

$$\Delta = -h\nu_{AO} - KE^2 \tag{21}$$

where the shift rate is

$$K = -\tfrac{1}{2}\{\alpha_0(nS_{1/2}) - \alpha_0(6P_{3/2}) - \alpha_2(6P_{3/2})\} \tag{22}$$

Δ was plotted versus the electric field squared, as is shown in Fig. 14. A line was fit to the data and the field such that atoms in the field-free and field regions were simultaneously in resonance, i.e., $\Delta = 0$ was found.

The polarizabilities $\alpha_0(nS_{1/2})$ were found using the small contributions of $\alpha_0(6P_{3/2}) = 407$ and $\alpha_2 = -65.1$ kHz/(kV/cm)^2 calculated by Zhou and Norcross (1989). The results listed in Table V agree with those found

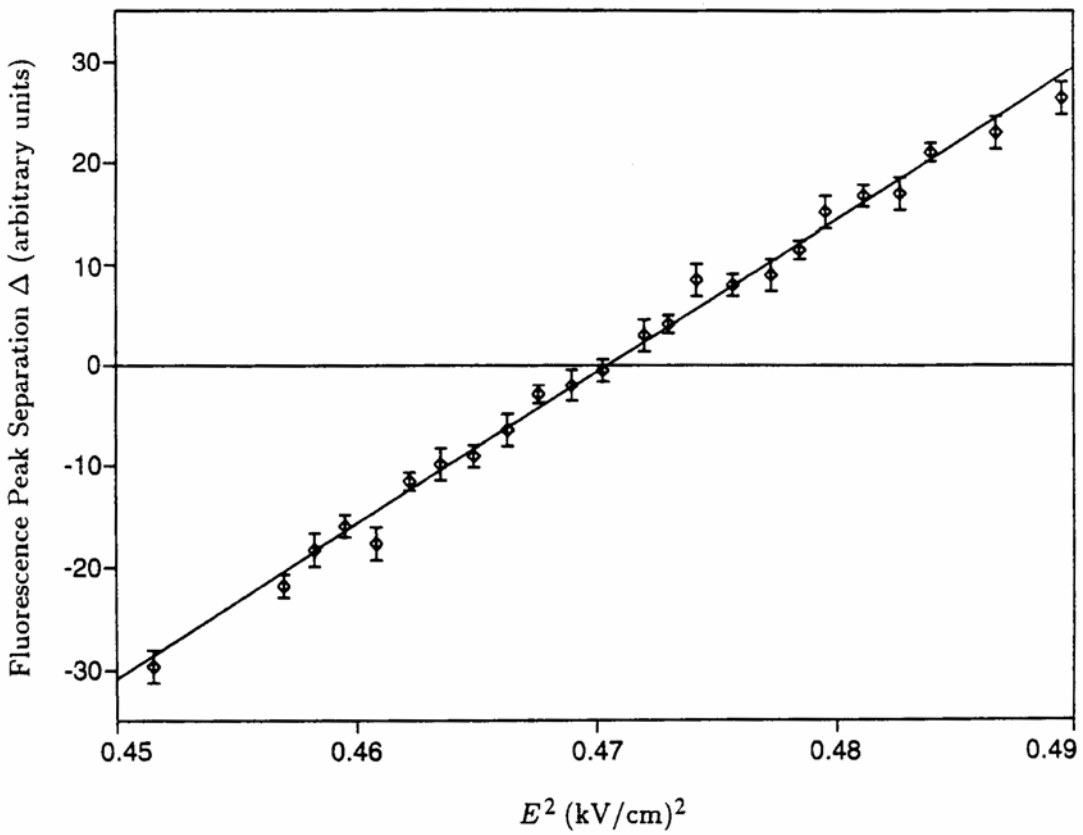

FIG. 14. Frequency separation Δ of fluorescent peaks observed in field and field-free regions versus electric field squared for excitation of the cesium $13S_{1/2}$ state using an acousto-optic modulation frequency of 350 MHz (van Wijngaarden *et al.*, 1994, by permission).

TABLE V
SCALAR POLARIZABILITIES OF THE CESIUM $(10-13)S_{1/2}$ STATES

	$\alpha_0(nS_{1/2})$ MHz/(kv/cm)^2		
n	Fredriksson and Svanberg (1977)	van Wijngaarden *et al.* (1994)	Theory
10	123 ± 6	119.06 ± 0.28	118
11	322 ± 16	309.70 ± 0.26	309
12	720 ± 45	713.48 ± 0.58	709
13	1650 ± 170	1491.20 ± 1.22	1490

by Fredriksson and Svanberg (1977) but are much more accurate. The latter group used a lamp that excited atoms in an atomic beam to the $6P_{3/2}$ state. The $6P_{3/2} \rightarrow (10-13)S_{1/2}$ transitions were excited by a dye laser having a linewidth of about 75 MHz. Data was taken at fixed dye laser frequency as follows. The electric field applied across the atomic beam was increased from 0 to a maximum of 7 kV/cm while fluorescence produced from the radiative decay of the excited $nS_{1/2}$ state was monitored by a photomultiplier. Flourescent peaks occurred whenever the dye laser excited one of the hyperfine levels of the $6P_{3/2}$ state to the Stark-shifted $nS_{1/2}$ state. The Stark shift rate was then found using the hyperfine splittings of the $6P_{3/2}$ state along with the field strengths corresponding to the peak maxima. The experimental accuracy was limited by uncertainties in the electric field determination and by the accuracy of the hyperfine data of the $6P_{3/2}$ state then available.

The data listed in Table V agree closely with results computed using the method developed by Bates and Damgaard (1949). These results were found using experimentally measured energies and assuming a Coulomb potential to describe the interaction of the valence electron and the nucleus plus the inner core electrons. This approximation has been used to compute polarizabilities in several alkali atoms (Gruzdev *et al.*, 1991; van Wijngaarden and Li, 1994c), and good agreement with the experimental data has been obtained for all but the lowest P states. This is not surprising since the Coulomb approximation best describes excited states that have minimal penetration of the inner electron core and have a small spin–orbit interaction.

D. CESIUM D LINES

Several groups have studied the Stark shifts of the $6S_{1/2} \rightarrow 6P_{1/2,3/2}$ transitions in cesium. Hunter *et al.* (1988) used two glass cells loaded with

cesium atoms. One cell was also filled with 6 Torr of nitrogen gas that pressure shifted the cesium resonance by 40 MHz. The second cell was made by gluing two metal plates onto a pyrex cylinder. These plates served as the electrodes that generated an electric field. The fluorescence signal observed by a photodiode in the pressurized cell was used to lock the laser to the transition frequency. An acousto-optic modulator shifted part of the laser beam by 40 MHz. The frequency-shifted laser beam was incident on the second cell, across which an electric field was applied. The modulation frequency needed for the laser to excite the Stark-shifted resonance was measured at various electric field strengths. Data were taken at laser powers of about 1 μW to minimize ac Stark shifts, optical pumping, and saturation effects.

The result for the D_1 line Stark shift is listed in Table VI. The $6S_{1/2} \rightarrow 6P_{3/2}$ transition was excited to the various hyperfine levels of the excited state to determine the tensor polarizability $\alpha_2(6P_{3/2})$. The experiment was done using a ring dye laser and repeated with a diode laser. The diode laser experienced slightly less frequency jitter and therefore produced data having a smaller statistical variation. The experimental accuracy was limited by the determination of the electric field. The cells were plagued with systematic uncertainties including leakage currents and needed to be coated with surfa-sil to minimize field inhomogeneities. Unfortunately, the coatings deteriorated noticeably after several months.

Tanner and Wieman (1988a) studied the Stark shift of the $6S_{1/2} \rightarrow 6P_{3/2}$ transition using apparatus similar to that shown in Fig. 10. An atomic beam passes through two plates that were separated by 0.3950 ± 0.0002 cm. One plate had a transparent conductive coating that permitted the laser to be transmitted, whereas the second plate was a gold-coated mirror. Electric fields were generated by applying voltages of up to 18 kV to the plates. Voltages were determined using a high voltage divider and a digital voltmeter. The divider drifted slightly with temperature, limiting the fractional uncertainty of the voltage calibration to 6×10^{-4}. The diode laser frequency was locked to the cesium resonance using a saturation signal observed in a cell. Part of the laser was frequency shifted by an acousto-optic modulator and excited the atoms passing between the field plates. The Stark shift was determined by measuring the modulation frequency needed to keep the atoms in resonance. The result listed in Table VI is somewhat lower than that found by Hunter *et al.* but has a five times smaller uncertainty. The accuracy was limited by the determination of the electric field.

A very accurate measurement of the Stark shift of the D_1 line was done by Hunter *et al.* (1992) using the apparatus illustrated in Fig. 15. Two diode lasers excited the $6S_{1/2} \rightarrow 6P_{1/2}$ transition at 894 nm. One laser was

TABLE VI
PRECISION STARK SHIFT SUMMARY

Atom	Transition $l \rightarrow u$	Polarizability	Value (kHz/(kV/cm)^2)[a]	Reference
Ba	$(6s)^2\,{}^1S_0 \rightarrow (6s6p)^1P_1$	$\alpha_0(u) - 2\alpha_2(u) - \alpha_0(l)$	57.06 ± 0.12	Li and van Wijngaarden (1995a)
		$\alpha_2(u)$	−10.72 ± 0.10	Kreutztrager and von Oppen (1973)
		$\alpha_2(u)$	−10.79 ± 0.29	Hese *et al.* (1977)
Ca	$(4s)^2\,{}^1S_0 \rightarrow (4s4p)^3P_1$	$\alpha_0(u) - 2\alpha_2(u) - \alpha_0(l)$	24.628 ± 0.082	Li and van Wijngaarden (1996)
Cs	$6S_{1/2} \rightarrow 7S_{1/2}$	$\alpha_0(u) - \alpha_0(l)$	1420.6 ± 4.8	Watts *et al.* (1983)
	$6S_{1/2} \rightarrow 6P_{1/2}$	$\alpha_0(u) - \alpha_0(l)$	241.2 ± 2.4	Hunter *et al.* (1988)
		$\alpha_0(u) - \alpha_0(l)$	230.44 ± 0.03	Hunter *et al.* (1992)
		$\alpha_0(u) - \alpha_0(l)$	230.5	Zhou and Norcross (1989)
	$6S_{1/2} \rightarrow 6P_{3/2}$	$\alpha_0(u) - \alpha_0(l)$	314.2 ± 3.2	Hunter *et al.* (1988)
		$\alpha_0(u) - \alpha_0(l)$	308.6 ± 0.6	Tanner and Wieman (1988a)
		$\alpha_0(u) - \alpha_0(l)$	308.0	Zhou and Norcross (1989)
		$\alpha_2(u)$	−64.7 ± 2.0	Hunter *et al.* (1988)
		$\alpha_2(u)$	−65.3 ± 0.4	Tanner and Wieman (1988a)
		$\alpha_2(u)$	−65.1	Zhou and Norcross (1989)
	$6P_{3/2} \rightarrow 10S_{1/2}$	$\alpha_0(u) - \alpha_0(l)$	118,720 ± 280	van Wijngaarden *et al.* (1994)
	$6P_{3/2} \rightarrow 11S_{1/2}$	$\alpha_0(u) - \alpha_0(l)$	309,360 ± 260	van Wijngaarden *et al.* (1994)
	$6P_{3/2} \rightarrow 12S_{1/2}$	$\alpha_0(u) - \alpha_0(l)$	713,140 ± 580	van Wijngaarden *et al.* (1994)
	$6P_{3/2} \rightarrow 13S_{1/2}$	$\alpha_0(u) - \alpha_0(l)$	1,490,900 ± 1200	van Wijngaarden *et al.* (1994)
K	$4S_{1/2} \rightarrow 4P_{1/2}$	$\alpha_0(u) - \alpha_0(l)$	78.800 ± 0.010	Miller *et al.* (1994)
Li	$2S_{1/2} \rightarrow 2P_{1/2}$	$\alpha_0(u) - \alpha_0(l)$	−9.243 ± 0.004	Hunter *et al.* (1991)
		$\alpha_0(u) - \alpha_0(l)$	−9.234 ± 0.082	Windholz *et al.* (1992)
		$\alpha_0(u) - \alpha_0(l)$	−9.272	Pipin and Bishop (1993)
	$2S_{1/2} \rightarrow 2P_{3/2}$	$\alpha_0(u) - \alpha_0(l)$	−9.281 ± 0.100	Windholz *et al.* (1992)
		$\alpha_2(u)$	0.408 ± 0.011	Windholz *et al.* (1992)

TABLE VI (*continued*)

Atom	Transition $l \rightarrow u$	Polarizability	Value (kHz/(kV/cm)^2)[a]	Reference
		$\alpha_2(u)$	0.399	Pipin and Bishop (1993)
Na	$3S_{1/2} \rightarrow 3P_{1/2}$	$\alpha_0(u) - \alpha_0(l)$	48.99 ± 0.11	Windholz and Neureiter (1985)
	$3S_{1/2} \rightarrow 3P_{3/2}$	$\alpha_0(u) - \alpha_0(l)$	49.28 ± 0.15	Windholz and Musso (1989)
		$\alpha_2(u)$	−21.97 ± 0.10	Windholz and Musso (1989)
		$\alpha_0(l)$	40.56 ± 0.14	Ekström *et al.* (1995)
Rb	$5S_{1/2} \rightarrow 5P_{1/2}$	$\alpha_0(u) - \alpha_0(l)$	122.306 ± 0.016	Miller *et al.* (1994)
Sm	$(4f^6 6s^2)\,^7F_1 \rightarrow$ $4f^6 6s6p + 4f^5 5d6s^2)\,^7F_1^0$	$\alpha_0(u) - \alpha_0(l)$	−91.8 ± 0.4	Neureiter *et al.* (1986)
		$\alpha_2(u) - \alpha_2(l)$	13.29 ± 0.06	Neureiter *et al.* (1986)
Yb	$(6s)^2\,^1S_0 \rightarrow (6s6p)\,^3P_1$	$\alpha_0(u) - 2\alpha_2(u) - \alpha_0(l)$	30.838 ± 0.096	Li and van Wijngaarden (1995b)
		$\alpha_2(u)$	5.81 ± 0.13	Li and van Wijngaarden (1995b)
		$\alpha_2(u)$	5.99 ± 0.34	Rinkleff (1980)
		$\alpha_2(u)$	6.04 ± 0.21	Kulina and Rinkleff (1982)

[a] Note that 1 kHz/(kV/cm)^2 = $4.0189 a_0^3/h$ and $a_0^3 = 1.4818 \times 10^{-25}$ cm^3, where a_0 is the Bohr radius and h is Planck's constant.

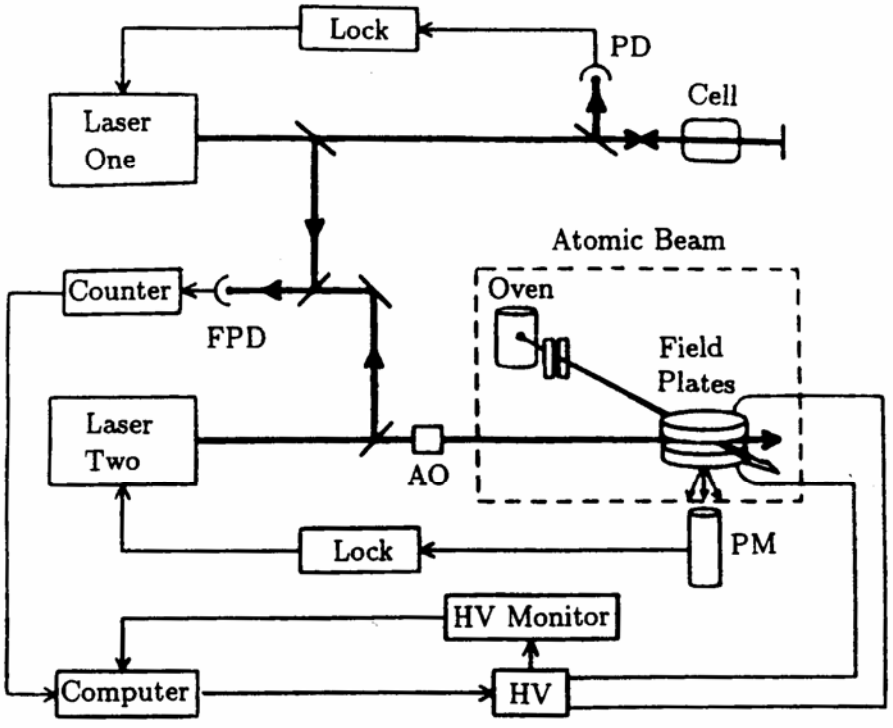

FIG. 15. Stark shift measurement apparatus for studying the alkali D lines (Hunter *et al.*, 1992, by permission).

locked to the D_1 line using the saturated absorption signal observed by a photodiode (PD) in a cell while the second laser excited an atomic beam as it passed through an electric field. Considerable care was spent designing the field electrodes to permit an accurate determination of the electric field. Two $\lambda/10$ optical quartz flats were coated with indium tin oxide, which has a transmission coefficient of over 80% at 894 nm. The fluorescence was therefore transmitted through the electrodes and detected by a photomultiplier (PM). The plate separation distance of about 2.8 mm was precisely determined using four 80% reflecting aluminium pads 2 mm in diameter that were placed at the corners of a 1.3-cm square centered on each electrode. The aluminium pads on the two electrodes were aligned to form four separate Fabry–Perot etalons. The electrode spacing could then be monitored throughout the experiment by measuring the free spectral range of the four etalons using a ring titanium sapphire (Coherent 899-21) laser and a wavemeter. This permitted the electrode spacing to be determined with a fractional uncertainty of 40 ppm. Voltages of up to ± 7.5 kV were applied to the plates. The voltage was determined using a high voltage divider chain accurate to 60 ppm that was constructed using

precision wire wound resistors. The reduced voltage was measured with a voltmeter to a precision of 30 ppm.

The experimental procedure was as follows. Part of the second diode laser was frequency shifted 60 MHz by an acousto-optic (AO) modulator. The frequency-shifted laser beam was then used to lock the diode laser to the Stark-shifted transition found by passing the atomic beam through the electric field. Part of each of the two diode laser beams was focused onto a fast photodiode (FPD). The acousto-optic modulator shifts the beat note to a higher frequency that is relatively insensitive to noise effects, which in general have lower frequency components. The beat frequency was measured by a counter as a function of the electric field to determine the Stark shift. Data were taken at various laser powers and voltages to check for systematic effects. The results given in Table VI are substantially more accurate than data found in their earlier experiment (Hunter *et al.*, 1988). Tanner and Wieman (1988a) also found results that were lower than those obtained by Hunter *et al.* (1988) in their study of the cesium D_2 line Stark shift. Hunter *et al.* (1992) attributed this discrepancy to an underestimate of the electric field uncertainty in their initial work. The improved experiment used an atomic beam instead of a cell for observing the Stark-shifted transition and therefore did not suffer from the various problems discussed earlier. Hunter *et al.* have also used diode lasers to study the Stark shifts of D_1 lines in lithium (Hunter *et al.* 1991), potassium, and rubidium (Miller *et al.*, 1994).

Several theoretical estimates of the D line Stark shifts have been made. The most accurate is that of Zhou and Norcross (1989), which is listed in Table VI. They used a semiempirical potential composed of a Thomas–Fermi potential plus a term describing the polarization of the inner electron core. The various potential parameters were adjusted to obtain optimum agreement of computed and measured excited state energies (Weber and Sansonetti, 1987). This potential was then used to solve the Dirac equation for the single valence electron. The close agreement between the calculated values and the measured results obtained for the Stark shifts of the D lines and the tensor polarizability of the $6P_{3/2}$ state is impressive.

E. Precision Stark Shift Summary

A summary of Stark shifts measured with uncertainties of less than 0.5% is given in Table VI. Many of these results have been found using experimental techniques that have already been presented and are therefore not further discussed. The group led by Windholz has studied a number of transitions in lithium (Windholz *et al.*, 1992), sodium (Windholz and

Neureiter, 1985), and samarium (Neureiter *et al.*, 1986). They used a ring dye laser to excite an atomic beam in a field-free region and in a uniform electric field. Fields of up to 300 kV/cm were generated by applying high voltages to stainless steel plates. Silver-coated optical glass flats could not be used as electrodes since the coatings were destroyed by occasional sparks at these high voltages. The laser frequency was scanned across the resonance, and the fluorescence was detected by photomultipliers. The change in laser frequency was monitored by passing part of the laser beam through a Fabry–Perot interferometer as is shown in Fig. 1. The accuracy of their results was limited to a few tenths of a percent by uncertainty in the frequency marker positions generated using the etalon. For the case of the lithium D_1 line, their data are in good agreement with the more accurate results found by Hunter *et al.* (1991). Both of the experimental determinations are a few percent lower than a theoretical estimate (Pipin and Bishop, 1993). The latter used a combined configuration interaction Hylleraas method to calculate wavefunctions and matrix elements.

An experiment by Ekström *et al.* (1995) used the recently developed technique of atom interferometry (Adams *et al.*, 1994) to determine the ground state polarizability of sodium. Their apparatus consists of a three-grating Mach–Zender interferometer. The transmission gratings have a 200-nm period and generated two atomic beams separated by 55 μm. One beam passed through an electric field created by applying a voltage across two metal foils. This generated a relative phase shift between the two beams given by

$$\Delta\phi = \frac{1}{\hbar v}\int_0^L \frac{\alpha_0 E^2}{2}\,dx \tag{23}$$

where v is the velocity of the atoms, α_0 is the ground state polarizability of sodium, E is the electric field, and L is the length of the electric field region. The two atomic beams were then recombined, and the resulting interference pattern was studied using a hot wire detector that was mounted on a translation stage. Phase shifts of up to 60 rad were observed using fields of several kV/cm.

The scalar polarizability $\alpha_0(3S_{1/2})$ was determined to be 40.56 ± 0.14 kHz/(kV/cm)^2. The uncertainty is due to statistical and systematic effects. The latter was dominated by geometrical effects such as fringing electric fields that affect the interaction length L. These were studied using electrode foils of 7 and 10 cm in length and using guard electrodes to minimize the fringing fields. Another complication was modeling the velocity distribution of the atoms in the atomic beam to estimate the average velocity v. The final result for $\alpha_0(3S_{1/2})$ is substantially better

than the value of 41.0 ± 2.9 kHz/(kV/cm)^2 (Hall and Zorn, 1974), which was determined by measuring the deflection of an atomic beam in an inhomogeneous electric field. The result obtained by the atom interferometric experiment can be combined with the measured Stark shifts of the sodium D lines (Windholz and Neureiter, 1985; Windholz and Musso, 1989) to obtain values of 89.55 ± 0.18 and 89.84 ± 0.19 kHz/(kV/cm)^2 for the scalar polarizabilities of the $3P_{1/2}$ and $3P_{3/2}$ states, respectively.

VI. Concluding Remarks

The technique of precisely measuring frequency shifts using acousto-optically modulated laser beams has been demonstrated in a number of experiments. The apparatus is relatively straightforward consisting of an atomic beam, a frequency-modulated laser beam, and a photomultiplier. Large fluorescence signals having little noise can be generated using either dye or diode lasers. The method has a number of advantages when compared with other techniques. It does not require large and very uniform magnetic fields, as are needed in level crossing and in optical double resonance experiments. The data analysis is also less complicated since only a Lorentzian or Gaussian function is fitted to the observed spectral line. Short temporal resolution using relatively expensive transient digitizers is also not required, as is the case in quantum beat spectroscopy. Most significantly, the frequency calibration is much simpler than using a Fabry–Perot etalon. Interferometers are plagued by numerous problems including vibrations and sensitivities to pressure and temperature fluctuations, necessitating the use of frequency-stabilized lasers locked to an atomic transition to stabilize the cavity. In contrast, computer-controlled frequency synthesizers can quickly and conveniently generate a much wider range of frequencies with an accuracy of one part per million.

Over the past decade, experiments using acousto-optically modulated lasers have yielded isotope, hyperfine, and Stark shifts representing frequency intervals ranging from a few megahertz to several gigahertz. Data of unprecedented accuracy with uncertainties as low as several parts in 10^5 have been obtained. These results pose a stringent test for theories of multielectron atoms. The measured Stark shifts can also be used in conjunction with data obtained using novel new methods such as atom interferometry to determine scalar polarizabilities of excited states that heretofore could not be determined. Hence, the method of using

frequency-modulated lasers is very versatile, and optical modulators are likely to play an increasingly important role in precision laser spectroscopy.

Acknowledgments

This work was supported by the Natural Sciences and Engineering Research Council of Canada and York University.

References

Abele, J. (1975). *Z. Phys.* **274**, 179.
Adams, C. S., Carnal, O., and Mlynek, J. (1994). *Adv. At. Mol. Opt. Phys.* **34**, 1.
Arimondo, E., Inguscio, M., and Violino, P. (1977). *Rev. Mod. Phys.* **49**, 31.
Baird, P. E. G., Brambley, R. J., Burnett, K., Stacey, D. N., Warrington, D. M., and Woodgate, G. K. (1979). *Proc. R. Soc. London, Ser. A* **365**, 567.
Bates, D. R., and Damgaard, A. (1949). *Philos. Trans. R. Soc. London* **242**, 101.
Baumann, M., and Wandel, G. (1966). *Phys. Lett.* **22**, 283.
Baumann, M., and Wandel, G. (1968). *Phys. Lett. A* **28A**, 200.
Baumann, M., Liening, H., and Wandel, G. (1969). *Z. Phys.* **221**, 245.
Beckmann, A., Boklen, K. D., and Elke, D. (1974). *Z. Phys.* **270**, 173.
Blundell, S. A., Johnson, W. R., and Sapirstein, J. (1991). *Phys. Rev. A* **43**, 3407.
Bonin, K. D., and Kadar-Kallen, M. A. (1993). *Phys. Rev. A* **47**, 944.
Bouchiat, M. A. (1991). *In* "Proceedings of the Twelfth International Conference on Atomic Physics, 1990" (J. C. Zorn and R. R. Lewis, eds.), p. 399. American Institute of Physics, New York.
Broadhurst, J. H., Cage, M. E., Clark, D. L., Greenlees, G. W., Griffith, J. A. R., and Isaak, G. R. (1974). *J. Phys. B* **7**, L513.
Buck, P., Rabi, I. I., and Senitzky, B. (1956). *Phys. Rev.* **104**, 553.
Budick, B., and Snir, J. (1967). *Phys. Lett. A* **24A**, 689.
Budick, B., and Snir, J. (1970). *Phys. Rev. A* **1**, 545.
Carlsson, J. (1988). *Z. Phys. D: At. Mol. Clusters* **9**, 147.
Carlsson, J., Jonsson, P., Sturesson, L., and Froese Fischer, C. (1992). *Phys. Scr.* **46**, 394.
Chaiko, Y. (1970). *Opt. Spectrosc.* **20**, 424.
Chamberlain, G. E., and Zorn, J. C. (1963). *Phys. Rev.* **129**, 677.
Clark, D. L., Cage, M. E., Lewis, D. A., and Greenlees, G. W. (1979). *Phys. Rev. A* **20**, 239.
Corney, A. (1977). "Atomic and Laser Spectroscopy." Clarendon Press, Oxford.
Deilamian, K., Gillaspy, J. D., and Kelleher, D. E. (1993). *J. Opt. Soc. Am. B* **10**, 789.
DeMille, D. (1995). *Phys. Rev. Lett.* **74**, 4165.
Dzuba, V. A., Flambaum, V. V., and Sushkov, O. P. (1989). *Phys. Lett. A* **140**, 493.
Ekström, C. R., Schmiedmayer, J., Chapman, M. S., Hammond, T. D., and Pritchard, D. E. (1995). *Phys. Rev. A* **51**, 3883.
Fredriksson, K., and Svanberg, S. (1977). *Z. Phys. A* **281**, 189.
Gaupp, A. Kuske, P., and Andrä, H. J. (1982). *Phys. Rev. A* **26**, 3351.
Griffith, J. A. R., Isaak, G. R., New, R., Ralls, M. P., and van Zyl, C. P. (1977). *J. Phys. B* **10**, L91.

Gruzdev, P. F., Soloveva, G. W., and Sherstyuk, A. I. (1991). *Opt. Spectrosc.* **71**, 513.
Hall, W. D., and Zorn, J. C. (1974). *Phys. Rev. A* **10**, 1141.
Hartmann, W. (1970). *Z. Phys.* **240**, 323.
Hese, A., Renn, A., and Schweda, H. S. (1977). *Opt. Commun.* **20**, 385.
Hoffnagle, J., Telegdi, V. L., and Weis, A. (1981). *Phys. Lett.* **86A**, 457.
Holmes, B. W., and Griffith, J. A. R. (1995). *J. Phys. B* **28**, 191.
Hunter, L. R., Krause, D., Murthy, S., and Sung, T. W. (1988). *Phys. Rev. A* **37**, 3283.
Hunter, L. R., Krause, D., Berkeland, D. J., and Boshier, M. G. (1991). *Phys. Rev. A* **44**, 6140.
Hunter, L. R. Krause, D., Miller, K. E., Berkeland, D. J., and Boshier, M. G. (1992). *Opt. Commun.* **94**, 210.
Jin, W. G., Horiguchi, T., Wakusugi, M., Hasegawa, T., and Yang, W. (1991). *J. Phys. Soc. Jpn.* **60**, 2896.
Johnson, W. R., Idrees, M., and Sapirstein, J. (1987). *Phys. Rev. A* **35**, 3218.
Kadar-Kallen, M. A., and Bonin, K. D. (1994). *Phys. Rev. Lett.* **72**, 828.
Kallas, K., Markova, G., Khvostenko, G., and Chaika, M. (1965). *Opt. Spectrosc.* **19**, 303.
Khadjavi, A., Lurio, A., and Happer, W. (1968). *Phys. Rev.* **167**, 128.
Korpel, A. (1988). "Acousto-Optics." Dekker, New York.
Kreutztrager, A., and von Oppen, G. (1973). *Z. Phys.* **265**, 421.
Kulina, P., and Rinkleff, R. H. (1982). *Z. Phys. A* **304**, 371.
Lawler, J. E., and Doughty, D. A. (1995). *Adv. At. Mol. Opt. Phys.* **34**, 171.
Li, J. (1995). Ph.D. Dissertation, York University, Toronto, Ontario, Canada (unpublished).
Li, J., and van Wijngaarden, W. A. (1995a). *Phys. Rev. A* **51**, 3560.
Li, J., and van Wijngaarden, W. A. (1995b). *J. Phys. B* **28**, 2559.
Li, J., and van Wijngaarden, W. A. (1996). *Phys. Rev. A* **53**, 604.
Lindgren, I., Lindgren, J., and Martensson, A. (1976). *Z. Phys. A* **279**, 113.
Mathur, B. S., Tang, H., and Happer, W. (1968). *Phys. Rev.* **171**, 11.
Miller, K. E., Krause, D., and Hunter, L. R. (1994). *Phys. Rev. A* **49**, 5128.
Miller, T. M., and Bederson, B. (1977). *Adv. At. Mol. Opt. Phys.* **13**, 1.
Miller, T. M., and Bederson, B. (1988). *Adv. At. Mol. Opt. Phys.* **25**, 37.
Molof, R. W., Schwartz, H. L., Miller, T. M., and Bederson, B. (1974). *Phys. Rev. A* **10**, 1131.
Neureiter, C., Rinkleff, R. H., and Windholz, L. (1986). *J. Phys. B* **19**, 2227.
Noecker, M. C., Masterson, B. P., and Wieman, C. E. (1988). *Phys. Rev. Lett.* **61**, 310.
Perl, M. L., Rabi, I. I., and Senitzky, B. (1955). *Phys. Rev.* **98**, 611.
Pescht, K., Gerhardt, H., and Matthias, E. (1977). *Z. Phys. A* **281**, 199.
Pipin, J., and Bishop, D. M. (1993). *Phys. Rev. A* **47**, R4571.
Rafac, R. J., Tanner, C. E., Livingston, A. E., Kukla, K. W., Berry, H. G., and Kurtz, C. A. (1994). *Phys. Rev. A* **50**, R1976.
Ramsey, N. F. (1956). "Molecular Beams." Oxford Univ. Press, London.
Rayman, M. D., Aminoff, C. G., and Hall. J. L. (1989). *J. Opt. Soc. Am. B* **6**, 539.
Rebhan, U., Wiegart, N. J., and Kunze, H. J. (1981). *Phys. Lett.* **85A**, 228.
Riis, E., Sinclair, A. G., Poulsen, O., Drake, G. W. F., Rowley, W. R. C., and Levick, A. P. (1994). *Phys. Rev. A* **49**, 207.
Rinkleff, R. H. (1980). *Z. Phys. A* **296**, 101.
Ross. J. S. (1963). *J. Opt. Soc. Am.* **53**, 299.
Salomonson, S., and Ynnerman, A. (1991). *Phys. Rev. A* **43**, 88.
Schmidt-Kaler, F., Leibfried, D., Weitz, M., and Hänsch, T. W. (1993). *Phys. Rev. Lett.* **70**, 2261.
Schmoranzer, H., Schulze-Hagenest, D., and Kandela, S. A. (1979). *Symp. At. Spectrosc. Sept. 1979*, p. 195. Tucson, AZ.
Svanberg, S., and Belin, G. (1972). *Z. Phys.* **251**, 1.

Svanberg, S., and Rydberg, S. (1969). *Z. Phys.* **227**, 216.
Tanner, C. E., and Wieman, C. (1988a). *Phys. Rev. A* **38**, 162.
Tanner, C. E., and Wieman, C. (1988b). *Phys. Rev. A* **38**, 1616.
Tran, C. D. (1992). *Anal. Chem.* **64**, 971.
Umfer, C., Windholz, L., and Musso, M. (1992). *Z. Phys. D: At. Mol. Clusters* **25**, 23.
van Wijngaarden, W. A., and Li, J. (1994a). *J. Opt. Soc. Am. B* **11**, 2163.
van Wijngaarden, W. A., and Li, J. (1994b). *Z. Phys. D: At. Mol. Clusters* **32**, 67.
van Wijngaarden, W. A., and Li, J. (1994c). *J. Quant. Spectrosc. Radiat. Transfer* **52**, 555.
van Wijngaarden, W. A., and Li, J. (1995). *Can. J. Phys.* **73**, 484.
van Wijngaarden, W. A., Bonin, K., Happer, W., Miron, E., Schreiber, D., and Arisawa, T. (1986). *Phys. Rev. Lett.* **56**, 2024.
van Wijngaarden, W. A., Hessels, E. A., Li, J., and Rothery, N. E. (1994). *Phys. Rev. A* **49**, R2220.
Violino, P. (1969). *Can. J. Phys.* **47**, 2095.
Walther, H. (1974). *Phys. Scr.* **9**, 297.
Wandel, G. (1970). *Z. Phys.* **231**, 434.
Watts, R. N., Gilbert, S. L., and Wieman, C. E. (1983). *Phys. Rev. A* **27**, 2769.
Weber, K. H., and Sansonetti, G. (1987). *Phys. Rev. A* **35**, 4650.
Windholz, L., and Musso, M. (1989). *Phys. Rev. A* **39**, 2472.
Windholz, L., and Neureiter, C. (1985). *Phys. Lett.* **109A**, 155.
Windholz, L., Musso, M., Zerza, G., and Jager, H. (1992). *Phys. Rev. A* **46**, 5812.
Xu, J., and Stroud, R. (1992). "Acousto-Optic Devices." Wiley, New York.
Young, T. P., and Griffith, J. A. R. (1994). *Tech. Dig. European Quantum Electronics Conference, 1994*, Amsterdam.
Zhao, P., Lawall, J. R., and Pipkin, F. M. (1991). *Phys. Rev. Lett.* **66**, 592.
Zhou, H. L., and Norcross, D. W. (1989). *Phys. Rev. A* **40**, 5048.